11

FABRICATION AND APPLICATIONS OF CARBON/CLAY MINERAL NANOCOMPOSITES

Bin Mu, Aiqin Wang

Key Laboratory of Clay Mineral Applied Research of Gansu Province, Center of Eco-material and Green Chemistry, Lanzhou Institute of Chemical Physics, Chinese Academy of Sciences, Lanzhou, People's Republic of China

11.1 Carbon Materials and Clay Minerals

Carbon materials as attractive and fascinating families are assuredly the "dazzling stars" in the field of material science due to their unique structure, excellent properties, and diverse morphologies, including zero-dimensional (i.e., fullerene, carbon quantum dots, and carbon onion), one-dimensional (i.e., carbon nanotube, carbon nanofiber), two-dimensional (i.e., graphene, three-dimensional carbon aerogel), and the disordered or amorphous carbon (i.e., activated carbon, biochar) (Fig. 11.1A). Although carbon materials have been widely applied in various fields, such as electrochemical energy storage [1, 2], environmental science (e.g., purification, remediation) [3, 4], catalysis [5, 6], and biomedicine applications [7] due to their unique properties, some disadvantages severely restrict their feasible applications in practice, such as high costs, complex preparation process, low yield, and even harsh preparation conditions (high temperature and vacuum). In the case of the application of carbon materials in the environmental field, the break-even price of the biochar is about US \$246 t^{-1}, which is 1/6 of the price of commercial-activated carbon. Therefore, it is usually costly to remove pollutants using carbon materials as adsorbents in the environmental field [8].

Clay minerals are natural hydrous magnesium- or aluminum-rich phyllosilicates with diverse morphologies (Fig. 11.1B), such as one-dimensional sepiolite nanofibre, attapulgite (also called palygorskite), nanorod, halloysite nanotube, two-dimensional kaolinite, serpentine,

Nanomaterials from Clay Minerals. https://doi.org/10.1016/B978-0-12-814533-3.00011-9
© 2019 Elsevier Inc. All rights reserved.

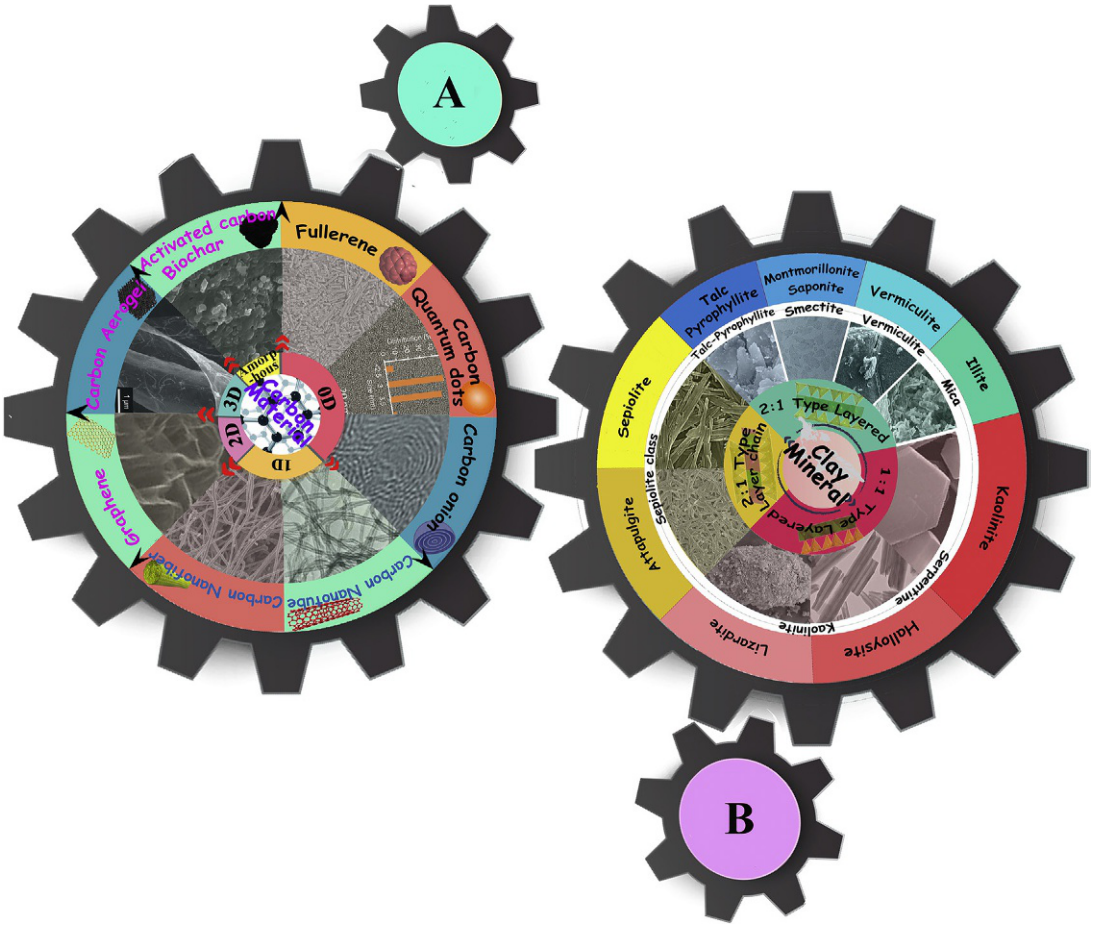

Fig. 11.1 The representative carbon materials (A) and clay minerals (B).

montmorillonite, vermiculite, and rectorite nanosheets. They have been proven to be the best candidates to match with carbon materials to form a variety of nanocomposites with potential applications in certain fields, especially in pollution control and environmental restoration because clay minerals have inherent advantages compared with carbon materials. These advantages include low costs, abundant reserves, high-specific surface area, nontoxic nature, and large ion-exchange capacity [9]. In order to improve the application performance of clay minerals, it is indispensable to modify clay minerals by using various physical or chemical methods, and incorporating carbon materials onto clay minerals may form new carbon/clay mineral nanocomposites with properties superior to individual components.

11.2 Preparation of Carbon/Clay Minerals Nanocomposites

In recent years, carbon/clay minerals nanocomposites have received growing attention, and numerous strategies have been employed to develop carbon/clay minerals nanocomposites. Based on the principle of strong noncovalent interaction between carbon nanotubes and clay minerals, multiwalled carbon nanotubes/montmorillonite hybrids [10], and multiwalled carbon nanotubes/sepiolite nanocomposites [11] have been prepared by a co-dispersion approach similar to steric stabilization in water after simply mixing pristine multiwalled carbon nanotubes in aqueous dispersion of montmorillonite or sepiolite. Using carbon nanotubes in aqueous medium without damaging the outer walls of carbon nanotubes during surfactant or oxidative treatments has proven to be very effective. Interestingly, the multiwalled carbon nanotubes/montmorillonite hybrids with different weight ratios also can be prepared by a simple dry grinding method [12], and the results indicated that a strong interaction occurred between multiwalled carbon nanotubes and montmorillonite while both of them were remarkably exfoliated in the as-prepared hybrids.

Pure fullerenes are insoluble in water and neutrally charged, so it is usually difficult to incorporate pure fullerenes into the interlayer galleries of clay minerals in aqueous solutions using the common ion exchange or intercalation methods. Tsoufis et al. first modified smectite using quaternary ammonium salt to increase the interlayer space and render the galleries organophilic, and then the organic solvent molecules derived from the fullerene solution entered into the galleries of smectite, transferring along the fullerene molecules. Thus the fullerene-pillared smectite nanocomposites were successfully obtained after selective removal of surfactant molecules by either ion-exchange reaction or thermal treatment [13]. In addition, carbon nanotube/clay minerals nanocomposites also could be synthesized in aqueous solution by a chemical reaction between their surface functional groups [14]. During this preparation process, kaolinite was first modified using hexamethylenediamine (HMDA) to obtain the organo-modified kaolinite, and meanwhile multiwalled carbon nanotubes were chemically oxidized by the mixture of HNO_3 and H_2O_2, and then the above materials were added into DMF and refluxed to produce carbon nanotube/kalolinite nanocomposites, as shown in Fig. 11.2. Furthermore, TEM image of the nanocomposites indicated no obvious agglomeration in the final bonding process, suggesting that the reaction occurred only on the surface of the particle. In addition to the above methods, the other strategies included chemical vapor deposition, hydrothermal carbonization, and high-temperature pyrolysis, which have also been

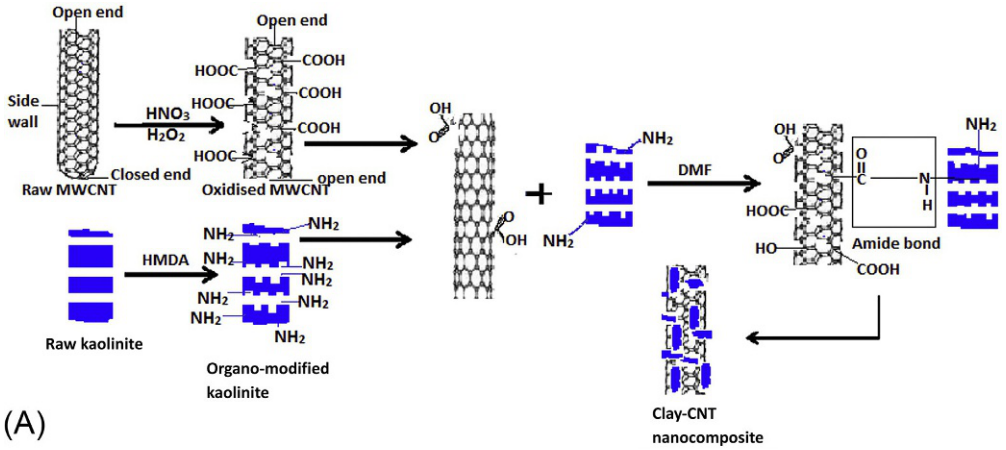

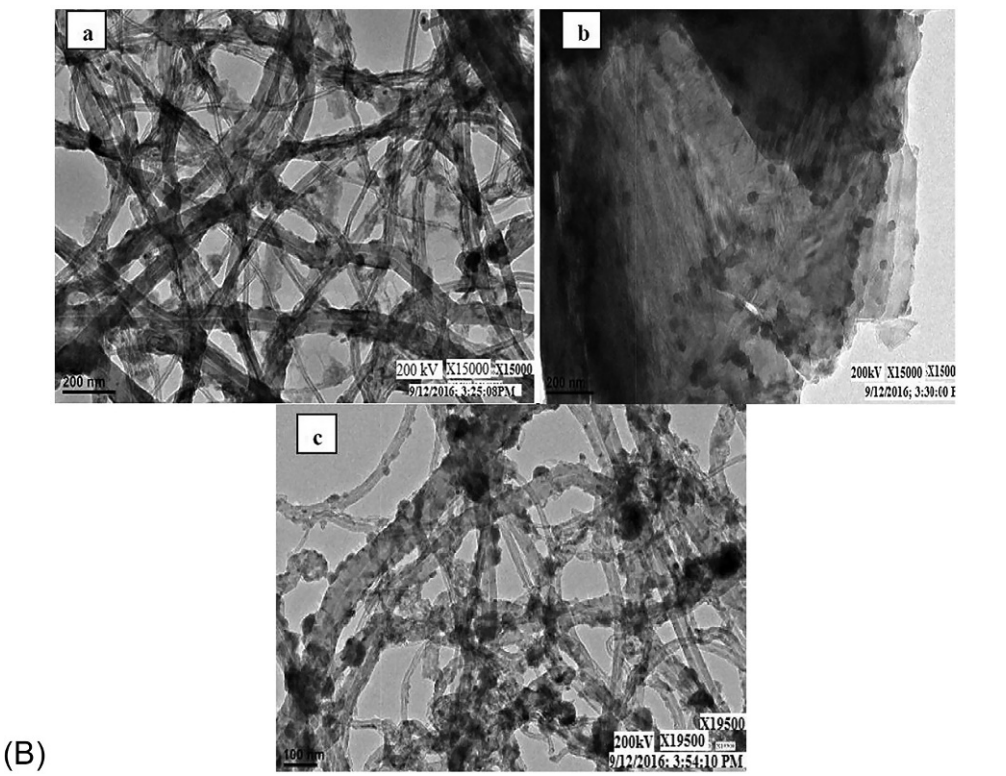

Fig. 11.2 (A) Schematic illustration for synthesis of carbon nanotube/kalolinite nanocomposites from chemically treated kalolinite and activated carbon nanotubes. (B) TEM images of (a) carbon nanotubes, (b) kalolinite and (c) the as-prepared nanocomposites. Reproduced with permission from V.B. Yadav, R. Gadi, S. Kalra, Synthesis and characterization of novel nanocomposite by using kaolinite and carbon nanotubes, Appl. Clay Sci. 155 (2018) 30–36.

used for the preparation of carbon/clay minerals nanocomposites with different structures, properties, and applications.

11.2.1 Chemical Vapor Deposition

Chemical vapor deposition is a classical deposition method to produce high quality and high-performance solid thin film materials, such as carbon nanotube, graphene, diamond, and metal [15, 16]. Therefore, this method was widely employed to grow carbon materials on the surface of clay minerals by chemical reaction and/or decomposition of volatile precursors [17]. Bakandritsos et al. successfully realized the growth of multiwalled carbon nanotubes on the surface of montmorillonite via chemical vapor deposition of acetylene after loading different amounts and types of metal salt catalyst precursors [18]. It was found that the anion of metal salt controlled the hydrolysis during metal deposition on the surface of montmorillonite and induced the transition to metal carbides during carbon deposition. Manikandan et al. systemically investigated the growth characteristics of carbon nanotubes on montmorillonite-supported iron catalysts by acetylene decomposition at various experimental conditions [19]. The results indicated selectivity toward carbon nanotubes increased with increases in the growth temperature. At lower temperatures, carbon deposits were mostly amorphous. Then they were replaced by crystalline carbon with increases in the temperature, and larger amounts of graphitic carbon structure were observed at 750°C rather than at 850°C due to the deactivation of acid sites on montmorillonite. When the growth experiments were carried out at the same carbon-feed ratio, the excessive carbon supply tended to deposit as amorphous carbon with the catalysts containing low concentration of iron oxide. On the contrary, either carbon nanotubes or graphitic carbon was formed at the catalysts, containing significant higher amounts of iron oxide. Under similar conditions, multiwalled carbon nanotubes or single-walled carbon nanotubes were also anchored on the surface of kaolinite, nontronite, and sepiolite [20, 21].

In addition, carbon nanotubes also can be confined to grow in the interlayer spacing of expandable clay minerals. For example, sponge-like exfoliated carbon nanotube/vermiculite hybrids with different contents of carbon nanotube were prepared by intercalating aligned carbon nanotube arrays into natural vermiculite interlayers for oil adsorption [22]. However, the chemical vapor deposition method has many disadvantages, for example, the precursors need to be volatile at near-room temperatures. Most of them are toxic, expensive, and dangerous accompanied with the generation of some hazardous matters, such as CO and HF. Therefore, it is hard to prepare carbon/clay minerals nanocomposites on a large scale by chemical vapor deposition.

11.2.2 Hydrothermal Carbonization

Hydrothermal carbonization is a chemical process for the conversion of organic compounds to structured carbon in an oxygen-free environment in the presence of subcritical water and autogenous pressure in the range of 2–10 MPa [23, 24]. The involved organics usually consist of monosaccharide, natural polysaccharides, and other organic molecules. Of particular importance, biomass for high value-added products was processed in recent years [25]. The obtained solid products were called hydrochar to distinguish it from biochar. Carbon/attapulgite nanocomposite adsorbent was fabricated by a one-pot hydrothermal carbonization process using glucose as the carbon source, which presented a high adsorption capacity for Cr(VI) and Pb(II) ions [26]. In the hydrothermal carbonization reaction process, incorporation of clay minerals could realize the modification by inducing the heterogeneous deposition of carbonaceous matters on their surfaces, and it facilitated to regulate the morphology and prevent the aggregation of hydrochar as well [27, 28].

Xu et al. systematically studied the morphology and adsorption properties of carbon/attapulgite nanocomposites prepared from different biomass carbon sources, including xylose, fructose, sucrose, and cellulose by a hydrothermal carbonization process [29]. Interestingly, it was found that the cellulose-derived carbon nanoparticles could be uniformly anchored on the surface of attapulgite, but xylose was carbonized to form free carbon microshperes. The fructose and sucrose were carbonized to form the coexistence phases of free carbon microspheres and attapulgite-loaded carbon nanoparticles. This phenomenon was attributed to the different material-feeding ratio resulting from the difference in the molecular weight of the involved biomass, which led to different carbon contents and the maximum adsorption capacities toward dye molecules. Furthermore, the carbon/halloysite nanocomposites were prepared using by a hydrothermal carbonization process that exhibited strong adsorption ability to protein, slow hemolysis rate, and low cytotoxicity in comparison with raw halloysite [30]. In other words, the as-prepared nanocomposites have good biocompatibility, and it is expected to be applied in biomedical areas such as drug-delivery vehicles.

11.2.3 Pyrolysis

Compared with the hydrothermal carbonization process, the pyrolysis process is more suitable and easily applied in industry. It often involves the thermo-chemical decomposition of organic compounds to produce various carbon-rich solids in the absence of oxygen or air [31]. According to the pyrolysis temperature, the resultant amorphous carbon can be classified into biochar prepared at low temperatures

(<700°C) and activated carbon obtained at high temperatures followed by an activation process. Based on the synergistic effect of clay minerals and amorphous carbon, it is a facile approach to directly calcine the clay minerals with organic compounds. Cellulosic biomass carbon/montmorillonite nanocomposites were successfully synthesized by a carbon-bed pyrolysis method [32]. The nanocomposite with granule-layer structure and less aggregation of carbon nanoparticles showed higher adsorption capacity to methylene blue (MB) than biomass carbon, and the adsorption capacity also increased with the increase in the content of montmorillonite. In addition, carbon/montmorillonite nanocomposites with high surface area were obtained by intercalating sugar into smectite and then calcining at 600°C in argon atmosphere [33], and the in situ generated graphene covered on the semctite surface to form a nanometric carbonaceous film, which exhibited excellent thermal stability and preserved the layered structure even at 900°C. Wang et al. also fabricated carbon/montmorillonite foam nanocomposites by direct carbonization of bismaleimide resin/organic montmorilonite mixtures at ambient pressure [34]. The pore walls of nanocomposites became thick, and the average pore sizes decreased with the increase in the added amount of organic montmorilonite. After adding 1.5 wt% of organo-montmorilonite, the bulk density, thermal conductivity, compressive strength, and modulus of the nanocomposites reached 0.35 $g\,cm^{-3}$, 0.108 $W\,m^{-1}\,K^{-1}$, 6.90 and 207 MPa, respectively.

Recently, Ruiz-Garcia's groups developed a facile strategy for the preparation of graphene-like supported on porous solids by two-steps using sucrose and gelatine as carbon precursors in the presence of sepiolite [35, 36]. In the case of sucrose, it was firstly in situ transformed into caramel on the external surface and within the nanochannel of sepiolite to form caramel-sepiolite nanocomposites after being microwave irradiated; then both of them were pyrolyzed at 800°C in an N_2 atmosphere to form carbon/sepiolite nanocomposites (Fig. 11.3A) [35]. TEM images of samples suggested that sepiolite was encapsulated by the discrete-formed carbonaceous material compared with that of the raw sepiolite (Fig. 11.3B). After the silicate component was etched, the coated carbonaceous materials still presented fibrous shape with small rounded particles, but the aggregated flake carbonaceous particles were obtained without the addition of sepiolite. This phenomenon also confirmed that the incorporation of sepiolite contributed to controlling the morphologies of the carbonaceous materials. Furthermore, carbon/sepiolite nanocomposites also presented a similar texture and morphology after being modified with silylating agents. In the case of gelatine, it spontaneously took place the assembly to sepiolite in the microwave irradiation step, which was different from that of using sucrose as carbon precursor [36]. However, the

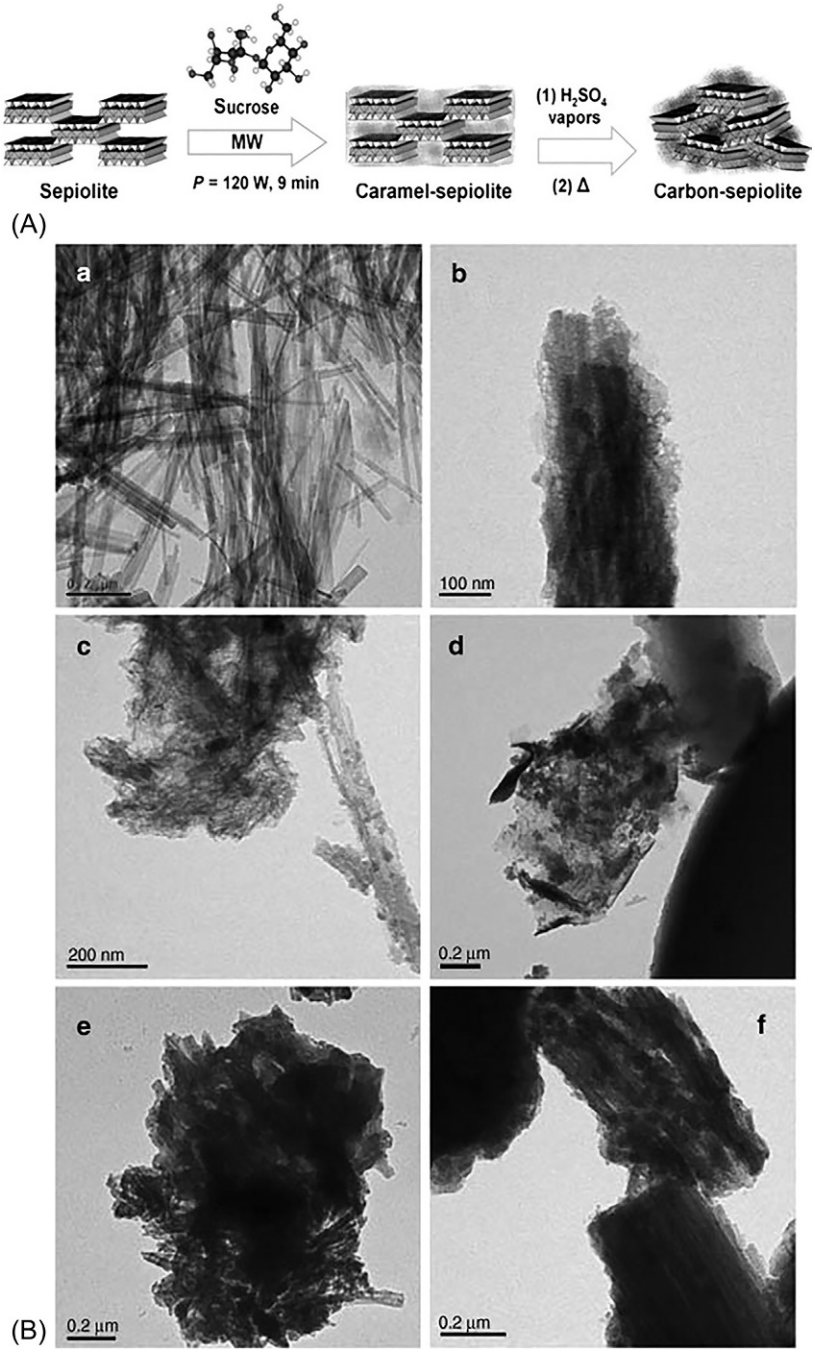

Fig. 11.3 (A) Schematic routes for the preparation of graphene supported on sepiolite using natural sucrose as carbon source. (B) TEM images of (a) sepiolite, (b) carbon/sepiolite nanocomposite, (c) carbonaceous materials derived from carbon/sepiolite nanocomposite, (d) sucrose-derived carbonaceous material, (e) and (f) silylating agents decorated nanocomposite. Reproduced with permission from E. Ruiz-Hitzky, M. Darder, F.M. Fernandes, E. Zatile, F.J. Palomares, P. Aranda, Supported graphene from natural resources: easy preparation and applications, Adv. Mater. 23 (2011) 5250–5255.

raw materials used in the above studies were relatively expensive, so it is essential to prepare carbon/clay minerals nanocomposites using cost-efficient carbon precursors.

The spent clay mineral-based adsorbents with loading of organics (i.e., dyes [37], antibiotic [38], and oil [39]) are promising candidates for constructing carbon/clay minerals nanocomposites by a simple pyrolysis process. Among the spent adsorbents, spent bleaching earth is particularly of interest due to the potential environmental and safety problems. In 2014, about 6,534,000 tons of the spent bleaching earth is only in China based on rough estimates, and its production is progressively increasing with the increase in consumption of edible oil all over the world. However, it is regretted that most of the spent bleaching earth does not obtain a reasonable and full recycling, and most of them are burned with coal or used as feed additives. Therefore, it may be an optimal choice to prepare carbon/clay minerals nanocomposites using the spent bleaching earth as the raw materials [40].

Our group has successfully prepared a series of carbon/attapulgite nanocomposites by a one-step carbonization process using the spent bleaching earth as the starting material [41–43]. Due to the cover of the residual organic matters on attapulgite, the spent bleaching earth powder exhibited dark brown powdery slag (Fig. 11.4A), and it was usually difficult to observe the rod shape morphology of attapulgite from the SEM image (Fig. 11.4E). After being calcined, the color of the products changed from black to gray with the increase in calcining temperatures from 250°C to 450°C (Fig. 11.4B–D), and the typical rod-like structure of attapulgite presented due to the carbonization of the residual organic matters (Fig. 11.4F–H). The nanocomposites obtained at 300°C exhibited high adsorption capacity and removal efficiency for organic pollutants and heavy metal ions compared with that of other calcining temperatures due to the synergistic effect of surface functional groups and pore structure parameters. This research is expected to provide a feasible approach to utilize the spent bleach earth with high added value and to develop high-efficient adsorbent for the decontamination of wastewater, oil bleaching, soil remediation, and others.

11.2.4 Hydrothermal Carbonization Associated With Pyrolysis

In order to improve the pore structural parameters and surface properties of carbon/clay mineral nanocomposites, a pyrolysis activation process often is conducted after hydrothermal carbonization [44]. Carbon hybridized montmorillonite nanosheets were prepared by combining hydrothermal carbonization of sucrose in the interlayer space of montmorillonite with pyrolysis at 800°C [45]. As shown

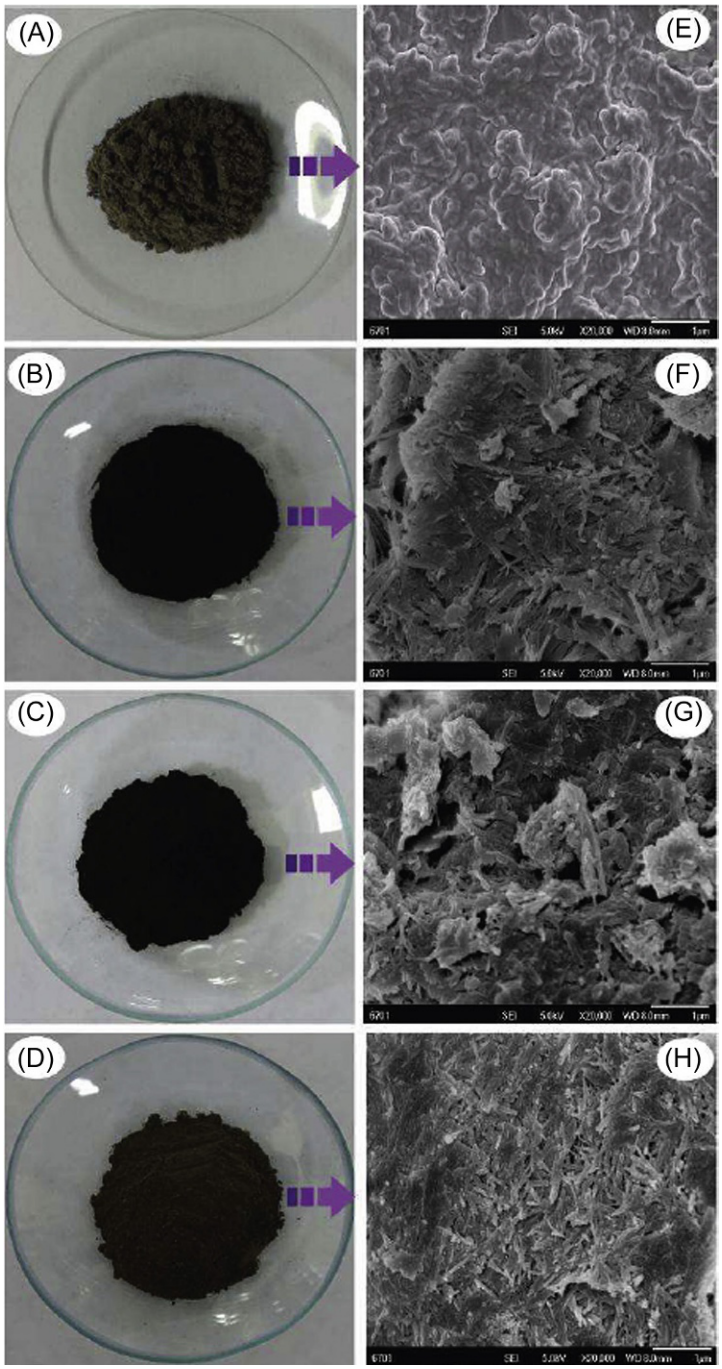

Fig. 11.4 Digital photographs and SEM images of (A) and (E) spent bleaching earth, (B)–(D) and (F)–(H) carbon/attapulgite obtained at 250°C, 300°C, and 450°C, respectively. Reproduced with permission from J. Tang, B. Mu, L. Zong, M.S. Zheng, A.Q. Wang, Fabrication of attapulgite/carbon composites from the spent bleaching earth for the efficient adsorption of methylene blue, RSC Adv. 5 (2015) 38443–38451.

in Fig. 11.5A and B, the original montmorillonite presented a typical two-dimensional nanosheet. After being hydrothermally treated in the presence of sucrose, the resultant hydrochar with loose flakes was intercalated into the interlayer space of montmorillonite (Fig. 11.5C), and a porous layered morphology was formed with the continuous calcining (Fig. 11.5E). However, only microspheres produced at the same hydrothermal conditions in the absence of montmorillonite. As shown in TEM images (Fig. 11.5D), montmorillonite was covered with amorphous hydrochar after the hydrothermal process, and then the hydrothermal carbon transformed into microcrystal carbon while the morphology of montmorillonite was still retained (Fig. 11.5F) after high-temperature pyrolysis. During the activation process, some activating agents were introduced to form a large number of pores, resulting in an increase in the surface area and pore volume [46, 47].

Zhang et al. successfully prepared carbon/palygorskite nanocomposites using $ZnCl_2$ as an activating agent, and the BET surface area was 11-fold higher than the unactivated one [48]. The carbon/montmorillonite nanocomposites with high surface area were prepared via one-step integration with calcination and H_2SO_4 activation [49], and it was found that H_2SO_4 activation during pyrolysis, combined with a short-range scale templating effect of montmorillonite, was essential for enhancing specific surface area. Furthermore, nitrogen-doped porous-activated carbon/montmorillonite nanocomposites were prepared through hydrothermal carbonization of glucose on montmorillonite followed by carbonization with melamine and activation with KOH at high temperatures for high-performance supercapacitors [50].

In summary, whatever method is used to fabricate carbon/clay mineral nanocomposites with different clay minerals and different carbon sources, the reaction mechanism may be different, which results in the difference in the carbon content and physical-chemical properties of carbon/clay minerals nanocomposites; thus it is very important to choose the suitable means to design and prepare carbon/clay minerals nanocomposites according to the relevant applications.

11.3 Structure and Physicochemical Properties of Carbon/Clay Mineral Naonocomposites

Due to the different raw materials, clay minerals, and preparation conditions, the as-prepared carbon/clay minerals nanocomposites exhibit different morphologies, chemical compositions, surface properties, and porous structures. The morphologies of carbon/clay minerals nanocomposites are dependent on the morphologies of the involved

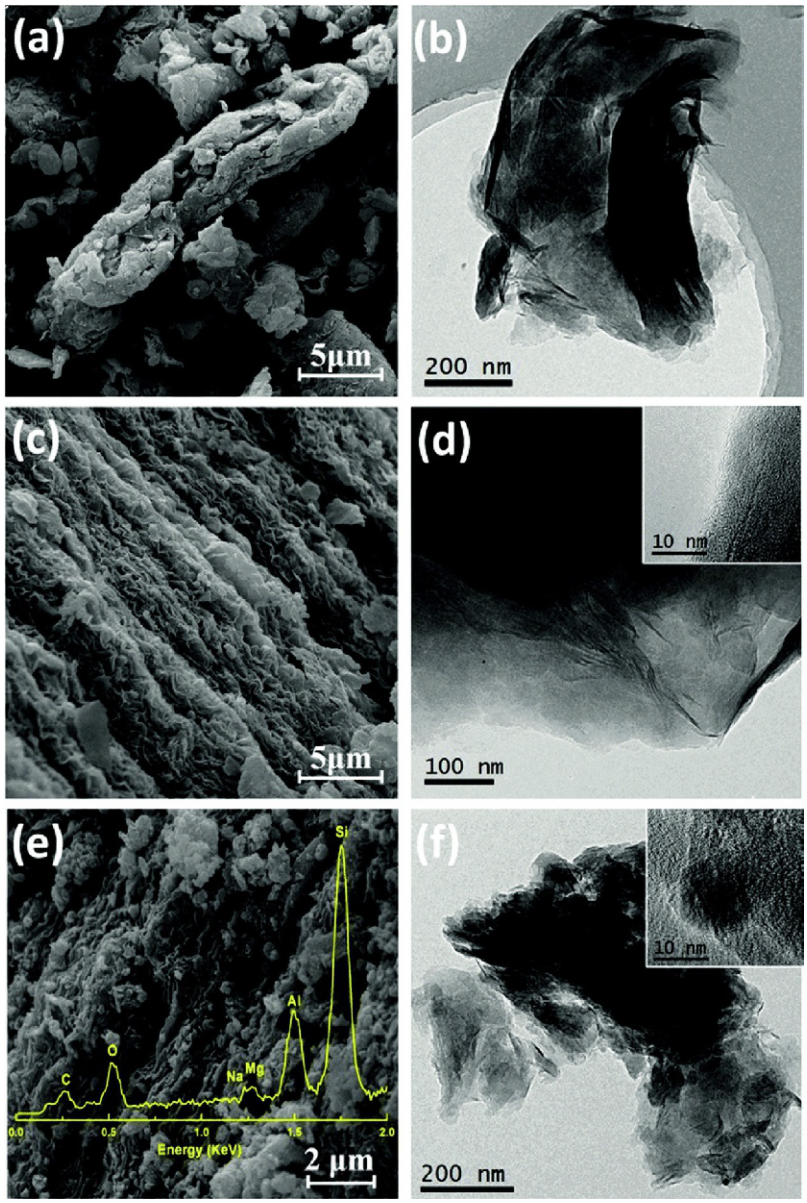

Fig. 11.5 SEM and TEM images of (A) and (B) montmorillonite, (C) and (D) hydrochar/montmorillonite nanocomposites, (E) and (F) carbon/montmorillonite nanocomposites, respectively. Reproduced with permission from K. Peng, H.M. Yang, Carbon hybridized montmorillonite nanosheets: preparation, structural evolution and enhanced adsorption performance, Chem. Commun. 53 (2017) 6085–6088.

clay minerals and the ratio of organic matters to clay minerals. The carbon/clay mineral nanocomposites may present one-dimensional or two-dimensional morphologies, in which the clay minerals were encapsulated with uniform carbon layer or carbon nanoparticles, and even accompanied with the presence of the free carbon microspheres at the high content of organic matters [28, 51]. Especially in

the hydrothermal process, the presence of clay minerals could effectively induce the heterogeneous deposition of carbonaceous matters on the surface of clay minerals to form well-defined nanostructured composites, preventing the usual homogeneous nucleation of carbon species from the bulk solution. On the contrary, only carbon microspheres were obtained in the absence of clay minerals [52]. The chemical compositions of carbon/clay minerals nanocomposites not only depend on the pyrolysis conditions, such as heating method, temperatures, time, and atmospheres, but also on the chemical composition of the organic matters on the surface, in the interlayer spacing, and inside the pore of clay minerals. Therefore, the main elements of carbon/clay mineral nanocomposites mainly consist of C, H, and O elements, sometimes heteroatoms originated from the loaded organic matters (N and S) [53], and Si, Mg, Al, Fe elements of clay minerals, and the content of these elements can be quantitatively determined by combining X-ray fluorescence techniques with elemental analysis.

The physicochemical properties of carbon/clay mineral nanocomposites depend on the textural (i.e., surface area and porosity) and surface chemical characteristics (i.e., acidic, basic, or neutral surface oxygen-containing groups), which is mainly determined by carbon materials [54]. The nature of the surface groups is usually identified using Fourier-transformed infrared spectroscopy and X-ray photoelectron spectroscopy, and their number can be determined quantitatively by selective titrations in aqueous solutions at room temperature [55]. In the case of the pore structure, carbon/clay minerals nanocomposites possess the hierarchical pore structures (micropore, mesopore, and miacropore) derived from clay minerals and the loaded carbon species, which can be measured by N_2 adsorption-desorption isotherms. In carbon/montmorillonite nanocomposites prepared by pyrolysis, clay mineral layers sustained the assembly of several graphene sheets for the creation of micropores, while other domains derived from "house of cards" arrangements provided mesoporosity or even macroporosity [49] (Fig. 11.6).

Furthermore, Sarkar et al. prepared two nanocomposites based on palygorskite and starch by hydrothermal carbonization technique with and without a postsynthesis heating activation treatment at 550°C for 3 h under CO_2 environment [56]. The results showed that the specific surface area of the nanocomposite prepared by heating activation treatment was 17-fold greater than that of the nanocomposite without treatment due to the formation of the graphitized carbon nanoparticles, micro- and mesopores structures after heating activation. However, the nanocomposite prepared without heating activation possessed large numbers of organic functional groups (C=H, C–C, C–O) and greater negative charge on its surface, which enabled it to generate a strong affinity with cationic dye molecules. On the contrary,

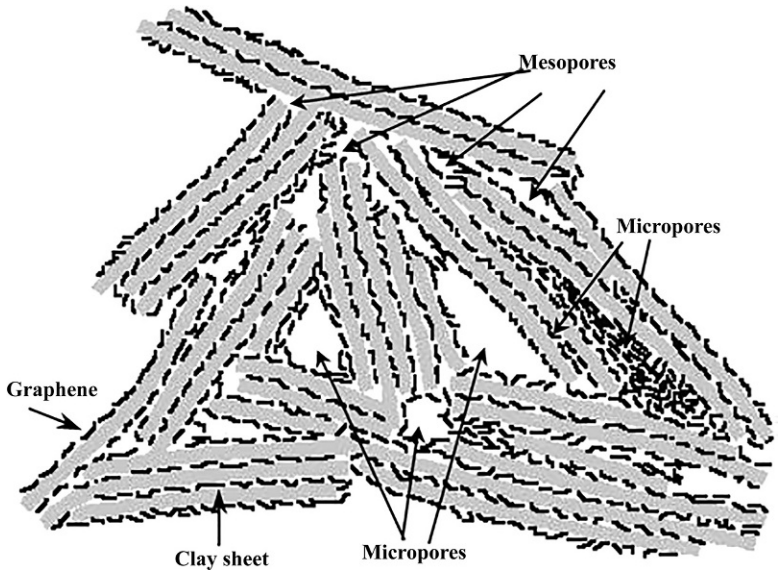

Fig. 11.6 Possible structure of carbon/montmorillonite nanocomposite. Reprinted with permission from A. Bakandritsos, T. Steriotis, D. Petridis, High surface area montmorillonite-carbon composites and derived carbons, Chem. Mater. 16 (2004) 1551–1559. Copyright (2004) American Chemical Society.

the heating-activated nanocomposites presented a strong affinity with anionic dyes, and the pore structures played a dominant role during the adsorption process. In a word, moderate heating activation treatment is favorable to improve the pore structure and surface properties of carbon/clay mineral nanocomposites, especially specific surface area, pore diameter, pore volume, and surface functional groups.

11.4 Applications of Carbon/Clay Mineral Nanocomposites

11.4.1 Environment Fields

The increasingly serious environmental pollution problems have aroused widespread attention over the world because a variety of pollutants have caused irreparable damage to eco-systems and human health. Among them, water pollution is especially concerning because the toxic pollutants in water, including heavy metal ions, dyes, pesticides, and antibiotics, have reached the point where it must be governed. Adsorption, as one of the most effective approaches to remove pollutants from water, is a stand out in many ways because of low-cost, high efficiency, ease of operation, and facile regeneration [57–60]. Therefore, much effort has been made to develop low-cost and high-performance adsorbents in the material, environmental science, and engineering fields. Carbon materials and clay minerals and their composites are potential adsorbents used to remove various

pollutants due to their advantages, including low-costs, ease of preparation, rich functional groups, large specific surface areas. The relevant research is making great progress.

11.4.1.1 Removal of Dyes

The dye effluents discharged from textile, paper, plastic, and leather industries may bring about serious water pollution and severe harm to human health and the safety of the ecosystem, even at very low concentrations <1 ppm for some dyes. Carbon/clay minerals composite adsorbents have received considerable attention because of their high efficiency to decontaminate dyeing wastewater. A series of carbon/palygorskite nanocomposites have been fabricated and used for the adsorption of dyes from aqueous solution [48, 61]. The activated carbon/palygorskite nanocomposite was prepared by a hydrothermal carbonization process of cellulose and palygorskite in the presence of ammonium ferrous iron sulfate and then activated by $ZnCl_2$. The resultant optimal product exhibited high BET specific surface area, large micropore surface area and micropore volume, and high adsorption capacity to MB (351 mg g^{-1}), which was far higher than that of carbon/palygorskite composites without activation using $ZnCl_2$ (89 mg g^{-1}). In comparison with conventional carbon sources, such as monosaccharide, disaccharide, polysaccharide, chitosan, and other organic matters, the carbon/palygorskite nanocomposites derived from one-step thermal treatment of spent bleaching earth, an abundant and cheap solid waste with loading of residual oil, have more potential to be used as cost-efficient adsorbents for removal of dyes from wastewater [42, 62].

Although a variety of adsorbents have been developed for removal of different pollutants, most adsorbents are difficult to separate from solutions. Compared with the traditional separation methods, such as filtration, sedimentation, and centrifugation, magnetic separation technology is a kind of simple, efficient, rapid, and inexpensive separation method [63, 64]. The magnetic carboxyl-functionalized carbon/attapulgite (carbon/APT) nanocomposites were prepared by a facile one-pot reaction process involved with the hydrothermal carbonization of organic matter, the redox reaction between the residual oils on spent bleaching earth or sodium citrate ($Na_3C_6H_5O_7{\cdot}2H_2O$) and Fe(III), and the precipitation of iron ions to generate iron-containing compounds (Fig. 11.7) [65]. During this preparation, all the reactions occurred simultaneously, and the dominant reaction and the properties of product (e.g., color, composition, morphology, magnetism, and adsorption capacity to dyes and heavy metal ions) were highly dependent on the sodium citrate concentration. The nanocomposites prepared at the sodium citrate concentration of 0.6 mol L^{-1} presented good adsorption capacity to MB (254.83 mg g^{-1}) and Pb(II)

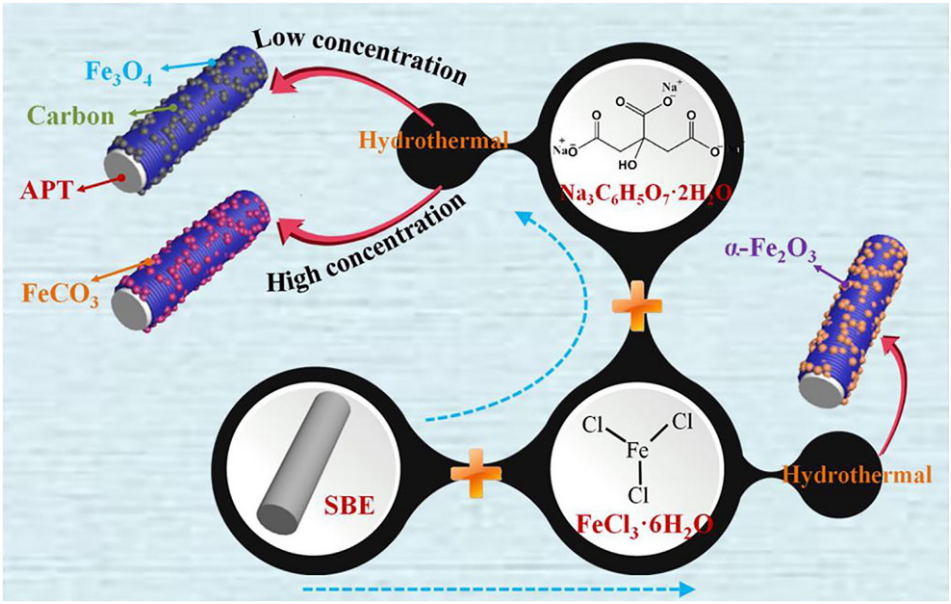

Fig. 11.7 Schematic illustration of the feasible mechanism for preparation of magnetic carboxyl-functionalized carbon/attapulgite nanocomposites. Reproduced with permission from J. Tang, B. Mu, L. Zong, M.S. Zheng, A.Q. Wang, Facile and green fabrication of magnetically recyclable carboxyl-functionalized attapulgite/carbon nanocomposites derived from spent bleaching earth for wastewater treatment, Chem. Eng. J. 322 (2017) 102–114.

(312.73 mg g^{-1}) because it integrated the advantages of attapulgite, carbon species, and iron-containing compounds. Furthermore, the adsorbent-loaded pollutants could be facilely separated from the solution after adsorption of the pollutants, and the adsorption capacity had no obvious decrease after six adsorption-desorption cycles. Based on a similar mechanism, the magnetic carbon/attapulgite supported NiFe layered double hydroxides were also fabricated via a hydrothermal method using spent bleaching earth as starting materials used for removal of pollutants [66]. The magnetic and adsorption properties of the as-prepared nanocomposites could be facilely controlled by varying the Ni/Fe molar ratio, and the optimal nanocomposites with a Ni/Fe molar ratio of 1:1 exhibited excellent adsorption capacities of 271.28, 180.90, and 308.21 mg g^{-1} for MB, Pb(II), and chlortetracycline hydrochloride, respectively.

As for the regeneration of adsorbents and the recovery of the adsorbed matters, the commonly used methods include chemical regeneration [67], supercritical fluid extraction [68], wet oxidation [69], electrochemical regeneration [70], and thermal treatment [71], etc. Most of them involve the use of chemicals (e.g., acid, alkali, or organic solvent), which may cause the risk of secondary pollution. Comparatively, thermally activated regeneration represents a

high-efficient and promising solution to recycling the spent adsorbents [72, 73]. More importantly, the continuous adsorption-calcination process can be used to construct carbon/clay minerals nanocomposites with increasing carbon content by the carbonization of organic matters adsorbed in each adsorption cycle, which is superior to the microwave-assisted regeneration process [74]. Therefore, our group investigated the continuous cyclic adsorption property of carbon/palygorskite nanocomposites by continuous adsorption-calcination process using methyl violet (MV) as a model pollutant [75]. The initial carbon/palygorskite composites with fast adsorption rate and excellent adsorption capacity of 239.34 mg g^{-1} to MV were first prepared by one-step calcination of spent bleaching earth after bleaching of animal fat. Then, the MV-loaded carbon/palygorskite nanocomposites were regenerated by thermal treatment at 500°C. The adsorption and thermal treatment process proceeded for 10 cycles, and it was interesting that no obvious decrease in the adsorption efficiency of the regenerated carbon/palygorskite nanocomposites was observed after 10 times consecutive adsorption-calcination cycles at the optimal temperature (Fig. 11.8). It was worth noting that this strategy also provided a feasible method to design and prepare carbon/clay mineral nanocomposites by cyclic utilization of various waste oils. Inspired by this strategy, carbon/attapulgite nanocomposites were successfully fabricated by calcining of the oil-loaded attapulgite at 300°C using waste hot-pot oil as a carbon source [76], which exhibited the excellent adsorption properties with the adsorption capacities of 215.83, 188.08, and 256.48 mg g^{-1} for MV, Pb(II) and tetracycline (TC), respectively (Fig. 11.9). The spent adsorbents after adsorption

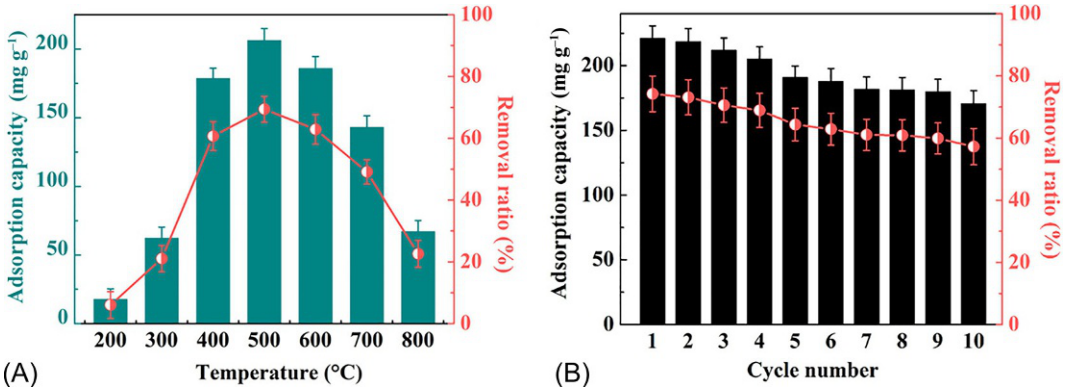

Fig. 11.8 (A) Effect of calcination temperature on the adsorption capacity of MV-loaded carbon/palygorskite nanocomposites and (B) the adsorption capacity of MV as a function of adsorption-calcination cyclic times. Reproduced with permission from J. Tang, L. Zong, B. Mu, Y.F. Zhu, A.Q. Wang, Preparation and cyclic utilization assessment of palygorskite/carbon composites for sustainable efficient removal of methyl violet, Appl. Clay Sci. 161 (2018) 317–325.

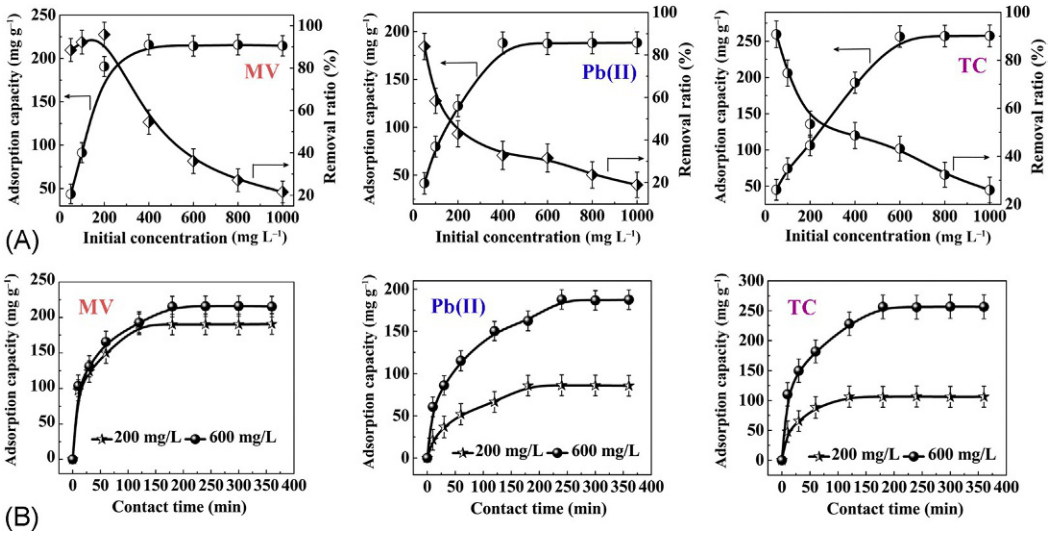

Fig. 11.9 Effect of (A) initial concentration and (B) contact time on the adsorption capacities of carbon/attapulgite nanocomposites for MV, Pb(II), and TC. Reproduced with permission from J. Tang, B. Mu, L. Zong, A.Q. Wang, From waste hot-pot oil as carbon precursor to development of recyclable attapulgite/carbon composites for wastewater treatment, J. Environ. Sci. 75 (2019) 346–358.

of MV and tetracycline could be thermally regenerated for recycling use. However, the MV- and TC-loaded spent adsorbents presented different pyrolysis behavior due to their different structures, and the optimum pyrolysis temperatures were 500°C and 300°C, respectively. No obvious decrease in the adsorption capacities of the regenerated adsorbents was found after 10 consecutive adsorption-calcination cycles for both MV and TC. The representative list of studies on the adsorption of dyes from wastewater using carbon/clay minerals nanocomposites as adsorbents was summarized in Table 11.1.

11.4.1.2 Removal of Heavy Metal Ions

Heavy metals are defined as metallic elements with a relatively high density compared with that of water, and most of them are harmful to human health and the ecosystem even at very low concentrations because they are toxic, easily mobile in the environment, bio-accumulated, and nondegradable in living tissues [86, 87]. The toxicity of heavy metal ions is usually related to several factors including dose and chemical species as well as physical conditions of the exposed individuals. In recent years, environmental contamination caused by heavy metal ions and their harm to human health has attracted increasing public concern worldwide. The reported sources of heavy metals in the environment include industrial, agricultural,

Table 11.1 A Representative List of Studies on the Adsorption of Dyes From Wastewater Using Carbon/Clay Minerals Nanocomposites

Raw Materials	Preparation Technique	Dyes	C_0 (mg L^{-1})	Q_{max} (mg g^{-1})	Reference
Spent bleaching earth	Pyrolysis/350–600°C	MB	31–500	42–45	[39]
Spent bleaching earth	Pyrolysis/300°C	MB	200	132.7	[42]
Montmorillonite and sucrose	Hydrothermal carbonization and pyrolysis/800°C	Congo red	1000	840.0	[45]
Cellulose and palygorskite	Hydrothermal carbonization and pyrolysis/$ZnCl_2$, 450°C	MB	300	351.0	[48]
Starch and palygorskite	Hydrothermal carbonization	MB	50	46.3	[56]
Cellulose and palygorskite	Hydrothermal carbonization	MB	10–100	22.28–37.79	[61]
Spent bleaching earth	Hydrothermal carbonization	MB	600	254.83	[65]
Spent bleaching earth	Hydrothermal carbonization	MB	400	271.28	[66]
Attapulgite and starch	Pyrolysis/300°C	MB, MV, MG	200	199	[74]
Spent bleaching earth	Pyrolysis/300°C	MV	300	239.3	[75]
Montmorillonite and glucose	Hydrothermal carbonization	MB	80	194.2	[77]
Attapulgite and rice hull	Pyrolysis/$ZnCl_2$, 500°C	Yellow X-GL	200	213.0	[78]
Bagasse and Montmorillonite	Pyrolysis/600°C	MB	20	11.3	[79]
montmorillonite and cellulose	Hydrothermal carbonization and pyrolysis/$ZnCl_2$, 400°C	MB	1000	686.94	[80]
Attapulgite and chiston	Hydrothermal carbonization	MB	200	226.24	[81]
Attapulgite and D-xylose	Hydrothermal carbonization	MB	60	181.0	[82]
Spent bleaching earth	Hydrothermal carbonization	Brilliant green	200	199.99	[83]
Spent dye-loaded palygorskite	Hydrothermal carbonization	MB MV	100	99.2 86.9	[84]
Bagasse and attapulgite	Pyrolysis/700°C	Brilliant red X-3B	200	72.2	[85]

pharmaceutical, domestic effluents, and atmospheric sources, especially mining, foundries and smelters, and other metal-based industrial operations [88]. Therefore, it is imperative to develop adsorbents to immobilize or remove heavy metal ions in addition to source pollution control.

Taken into account the synergistic effect of carbon materials and clay minerals, carbon/clay minerals nanocomposites have proved to be effective to remove heavy metal ions in recent years [89, 90]. The carbon/attapulgite nanocomposites prepared by low-temperature pyrolysis of spent bleach earth showed the maximum adsorption capacities of 32.32, 46.72, and 105.61 $mg\,g^{-1}$ for Cu(II), Cd(II) and Pb(II), respectively [41]. The formation of organic functional groups and biochar at low calcination temperatures was mainly responsible for the enhancement of adsorption properties to heavy metal ions, and the electrostatic interaction, cation exchange, and surface chemical complexation between Cd(II) and adsorbents were the main driving force of adsorption. However, the adsorption capacity of the obtained nanocomposites was lower than that of the adsorbent prepared by hydrothermal method. Recently, MnO_2-based adsorbents have been widely applied to remove heavy metal ions owing to their high natural abundance, high specific surface area, environmental compatibility, abundant surface functional groups, and strong affinities to heavy metal ions [91–93]. Its combination with carbon/palygorskite composites provides a new idea to fabricate new types of adsorbents. Our group also successfully fabricated manganese dioxide/carbon/attapulgite (MCA) ternary nanocomposites via a facile hydrothermal method based on spent bleaching earth [83]. During this process, the residual organic matter in spent bleaching earth was offered as a low-cost available carbon precursor as well as a reductant to induce the formation of manganese dioxide based on the redox reaction with $KMnO_4$. Interestingly, the initial concentration of $KMnO_4$ in the hydrothermal process was a dominant factor to affect the structures, components, and adsorption properties of ternary nanocomposites (Fig. 11.10), and the adsorption capacities toward brilliant green and Pb(II) reached 199.99 and 166.64 $mg\,g^{-1}$, respectively.

In addition, the introduction of organic functional groups into the carbon/clay minerals nanocomposites also contributed to increasing the adsorption capacity toward heavy metal ions. The carboxylate-functionalized carbon/montmorillonite, hydroxylated carbon/montmorillonite, and aminated carbon/montmorillonite nanocomposites were prepared by a hydrothermal carbonization process followed by a postmodification using H_2O_2, NaOH and ethane diamine, respectively, for removal of Pb(II) [94]. The results indicated that the adsorption properties of carbon/montmorillonite nanocomposites

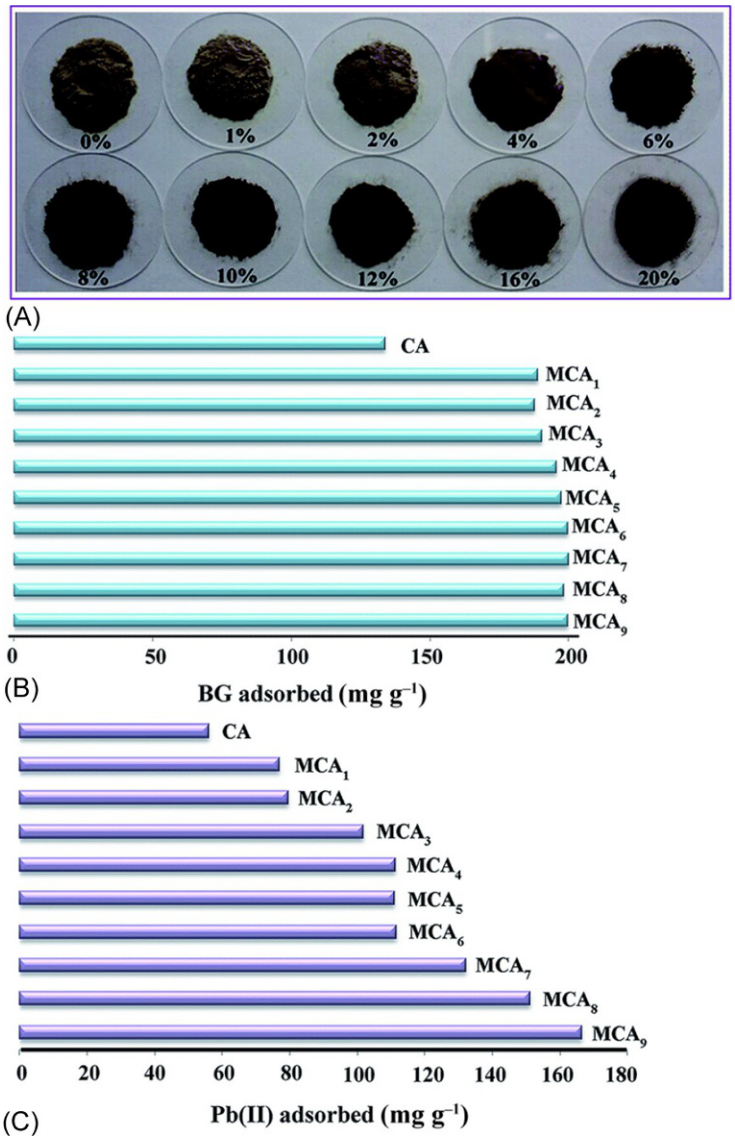

Fig. 11.10 (A) Digital photographs of ternary composites obtained after hydrothermal treatment at 140°C for 1 h at different initial $KMnO_4$ concentration, (B) and (C) effect of initial $KMnO_4$ concentration on adsorption capacity for brilliant green and Pb(II). Reproduced with permission from J. Tang, B. Mu, W.B. Wang, M.S. Zheng, A.Q. Wang, Fabrication of manganese dioxide/carbon/attapulgite composites derived from spent bleaching earth for adsorption of Pb(II) and brilliant green, RSC Adv. 6 (2016) 36534–36543.

toward Pb(II) were highly dependent on the surface functional groups, and the adsorption capacities followed the order of carboxylated carbon/montmorillonite > hydroxylated carbon/montmorillonite > aminated carbon/montmorillonite > carbon/montmorillonite, implying that the complexation of Pb(II) with functional groups, on the surface of adsorbents played an important role for removal of Pb(II), especially carboxyl groups. Our groups prepared magnetic carbon/attapulgite nanocomposites by simultaneous introduction of magnetic nanoparticles

and functional groups by the combination of one-pot hydrothermal carbonization and organo-modification processes using spent bleaching earth as raw materials [65, 66]. The resultant composites showed very good adsorption properties for heavy metal ions, which was superior to most other carbon/clay minerals nanocomposite adsorbents reported previously (Tables 11.2).

11.4.1.3 Other Organic Pollutants

Except for dye molecules, the common organic pollutants include pharmaceuticals, pesticides, interferon, and other chemicals. Antibiotics are an important family of drugs that have been used successfully for disease treatment and health protection. In recent years, antibiotics, especially those that have been banned such as streptomycin, gentamicin, and kanamycin, have also been widely used in animal feeding in large dosages to prevent disease and promote the growth of animals [100–102]. The excessive use of antibiotics not only results in the presence of drug-resistance bacteria, but their discharge also causes severe environmental contamination [103]. The adverse effects of the wide applications of antibiotics in human and veterinary medicines on the ecological environment have aroused ever-increasing attention. Therefore, it is urgent and significant to develop new types of adsorbents to efficiently remove antibiotics from water [104–106]. Due to the presence of multiple interactions between carbon materials and antibiotics, for example, hydrophobic effect, π-π interactions, hydrogen bonding, covalent, and electrostatic interactions [107], the low-cost carbon/clay minerals nanocomposites showed great application potentials for removal of antibiotics from aqueous solution [108, 109]. Our group prepared carbon/attapulgite nanocomposites by calcining spent bleaching earth, which showed the maximum adsorption capacities of 336.37 and 297.91 $mg\,g^{-1}$ for antibiotics chlortetracycline and tetracycline, respectively [38]. The spent adsorbents after adsorption of antibiotics can be regenerated by a simple calcination process, and the removal ratio of the regenerated adsorbents remained about 67.3% and 62.9% of the initial adsorption capacities for chlortetracycline and tetracycline, respectively, after 10 adsorption-calcining cycles.

Phenolic compounds are also discharged into the environment with various effluents produced from oil refining, petrochemical, pharmaceutical, coking operation, resin manufacturing, and plastic industries [110, 111]. Phenol has been designated as a priority pollutant by the US Environmental Protection Agency and the National Pollutant Release Inventory of Canada, and its harm to health is acute and chronic with numerous symptoms, such as anorexia, weight loss, irregular breathing, muscle weakness, tremor, and coma. Therefore, it is indispensable to decontaminate wastewater containing phenolic compounds before discharging into the environment [112]. Recently,

Table 11.2 A Representative List of Studies on the Adsorption of Heavy Metal Ions From Wastewater Using Carbon/Clay Minerals Nanocomposites as Adsorbents

Raw Materials	Preparation Methods	Heavy Metal	C_0 (mg L^{-1})	Q_{max} (mg g^{-1})	Reference
Attapulgite and glucose	Hydrothermal carbonization	Cr(VI)	100.35	177.74	[27]
		Pb(II)	164.60	263.83	
Illite and glucose	Hydrothermal carbonization	Cr(VI)	400	149.25	[29]
Spent bleaching earth	Pyrolysis/300°C	Cu(II)	200	32.32	[41]
		Pb(II)		105.61	
		Cd(II)		46.72	
Spent bleaching earth	Hydrothermal carbonization	Pb(II)	600	312.73	[65]
Spent bleaching earth	Hydrothermal carbonization	Pb(II)	400	180.90	[66]
Spent bleaching earth	Pyrolysis/400°C	Pb(II)	200	166.64	[83]
Sepiolite and glucose	Hydrothermal carbonization and pyrolysis/600°C	Pb(II)	200	28.04	[90]
Montmorillonite and D-glucose	Hydrothermal carbonization	Pb(II)	100	97.64	[94]
Glucose, ethylenediamine, and attapulgite	Hydrothermal carbonization	Cu(II)	250	125.4	[95]
Montmorillonite and glucose	Hydrothermal carbonization	U(VI)	9.15	20.76	[96]
Bentonite and water hyacinth	Pyrolysis/400°C	Cu(II), Pb(II)	200	78.1	[89]
				44.7	
Activated carbon and attapulgite	Physical blending	Cr(VI)	250	96.28	[97]
Attapulgite and graphene oxide	Physical blending	U(VI)	10	11.6	[98]
Montmorillonite and glucose	Hydrothermal carbonization	Cr(VI)	80	156.25	[99]

carbon/attapulgite nanocomposites were also developed and used to remove phenol [113, 114]. Wu et al. prepared well-defined core-shell carbon/clay minerals nanocomposites using cellulose and clay minerals (palygorskite, halloysite, and sepiolite) as starting materials, which showed good adsorption removal capability toward phenol [22, 28, 51]. It was well-known that acid treatment of the pristine sepiolite was in favor of increasing the specific surface area, density of silanol groups, and adsorption properties of sepiolite, which facilitated anchoring nanocarbon on the sepiolite surface. The carbon content in the carbon/sepiolite nanocomposite increased from 24.67 to 31.63 wt%, while the volume fraction of carbon increased from 45.5% to 57.8% after sepiolite was pretreated with acids. Comparatively, the pore volume and specific surface area of carbon/sepiolite nanocomposite were relatively lower than pristine sepiolite, but the adsorption capacity to phenol was higher 14.22-folds than pristine sepiolite due to the presence of nanocarbons with C=C, $-CH_2$, $-CH_3$, and C=O groups.

Recently, the petroleum pollution caused from oil spills brings a great risk for wildlife in the oceans and on the shores for a long time, and finally leads to substantial environmental and ecological problems. Therefore, many efforts have been devoted to develop high-performance and economical adsorbent materials for oil removal. It was proved that the adsorption capacities of vermiculite for diesel oil significantly enhanced to 26.7 $g\,g^{-1}$ after growing carbon nanotubes arrays on vermiculite layers [115]. More importantly, the adsorption capacity of carbon nanotube/vermiculite hybrids for diesel oil increased to 70.6 $g\,g^{-1}$ after being transformed into carbon nanotube/vermiculite fluffy by a high-speed shearing process, in which vermiculite sheets interlinked with the aligned carbon nanotubes bundles on both sides stacked together.

Table 11.3 summarized the representative researches about the adsorption of other organic pollutants from wastewater using carbon/clay minerals nanocomposites. As shown in Tables 11.1–11.3, the carbon/clay minerals nanocomposites exhibited good adsorption properties for most water pollutants, and it is possible to design special carbon/clay minerals nanocomposites according to the structures and properties of pollutant molecules required for removal.

11.4.2 Energy Storage

The increasing demand of global energy and the shortage of fossil fuel aroused great research interest on energy-saving and alternative clean energy worldwide [116, 117]. Li-ion batteries and supercapacitors as potential energy storage devices have been recognized as the most promising candidates for clean energy due to their higher power density over recyclable batteries, greater energy density than traditional

Table 11.3 The Adsorption Efficiency of Carbon/Clay Minerals Nanocomposites for Different Organic Pollutants

Raw Materials	Preparation Technique	Organic Pollutants	C_0 (mg L^{-1})	Q_{max} (mg g^{-1})	Reference
Sepiolite and CH_4	Chemical vapor deposition	Phenol	300	155.8	[20]
Sepiolite and cellulose	Hydrothermal carbonization	Phenol	200	14.22	[28]
Spent bleaching earth	Pyrolysis/300°C	Chlortetracycline tetracycline	600	336.4 297.9	[38]
Cellulose and halloysite	Hydrothermal carbonization	Phenol	5	5.23	[51]
Cellulose and halloysite	Hydrothermal carbonization/ pyrolysis, $ZnCl_2$,500°C	Phenol	5	33.3	[51]
Montmorillonite and wheat straw	Pyrolysis/400°C	Norfloxacin	150	25.53	[108]
Potato stem and attapulgite	Pyrolysis/500°C	Norfloxacin	20	5.24	[109]
Bentonite and sucrose	Pyrolysis/500°C, water vapor atmosphere	Phenol	507.2	110	[113]
Cellulose and palygorskite	Hydrothermal carbonization	Phenol	5	4.60	[114]
CNT arrays and vermiculite	Chemical vapor deposition	Diesel oil	–	26,700	[22]
Sodium carboxymethyl cellulose/montmorillonite	Pyrolysis/950°C	Waste pump oil	–	20,000	[115]

capacitors, as well as reliable cycle stability. The clay-supported carbon materials were proved to be a potential for energy storage because clay minerals could effectively induce the heterogeneous deposition of carbonaceous species on its surface and/or interlayer space, leading to the enhancement of electrochemical properties [50].

In order to enhance the electrochemical properties of carbon/clay minerals nanocomposites, the first strategy of activation treatment is utilized to enhance the specific surface area of carbon/clay minerals nanocomposites; the other one is to introduce the heteroatom or other electroactive components (metal oxides or conductive polymers). The carbon/attapulgite/polyaniline and carbon/halloysite/MnO_2 ternary nanocomposites were prepared by hydrothermal carbonization of glucose, followed by in situ chemical oxidative polymerization of aniline and the redox reaction between carbon and potassium permanganate, respectively [118, 119]. The synergistic effect of electroactive components obviously enhanced the electrochemical properties by integrating the merits of the individual component [120].

Graphene quantum dots (GQD) are a newly developed graphene family with good electrical conductivity and high theoretical capacitance, and thus GQD-halloysite nanotube (GQD-HNT) nanocomposites were developed for application in supercapacitor [121]. The GCD was anchored on the surface of HNT well by formation of amide linkage between the carboxylic groups of GCD and amine groups of the aminopropyltriethoxysilane modified HNT (APTES-HNT) (Fig. 11.11). Due to the utilization of high-charge storage sites and fast-ion transport characteristics, the obtained nanocomposites showed high specific capacitance of 63–216 $F\,g^{-1}$ at the current densities of 0.5–20 $A\,g^{-1}$ and energy density of 30–50 $Wh\,kg^{-1}$ for supercapacitor. After 5000 consecutive charge-discharge cycles at a current density of 6 $A\,g^{-1}$, the specific capacitance still retained 88% of the original capacitance. In addition, the graphene-like/sepiolite nanocomposities were directly used as electrode materials of rechargeable lithium batteries and supercapacitor without the addition of other conductive carbon [122, 123]. Interestingly, the nanocomposites modified with aminopropyltriethoxysilane at acidic condition may serve as conductive solid polyelectrolyte or transform into electrical conductors with ion recognition after being decorated with sulfonated organosilane [123].

Hydrogen is regarded as a predominant candidate of a future energy carrier for sustainable development. It is very crucial to develop a feasible on-board hydrogen storage system for hydrogen-powered fuel cell vehicles [124, 125]. Among various approaches to hydrogen storage, solid-state storage has received more attention because it may achieve the highest hydrogen density and the highest utility to the practical implementation of hydrogen storage. Therefore, the nanostructured materials with high-specific surface area and porosity are developed for

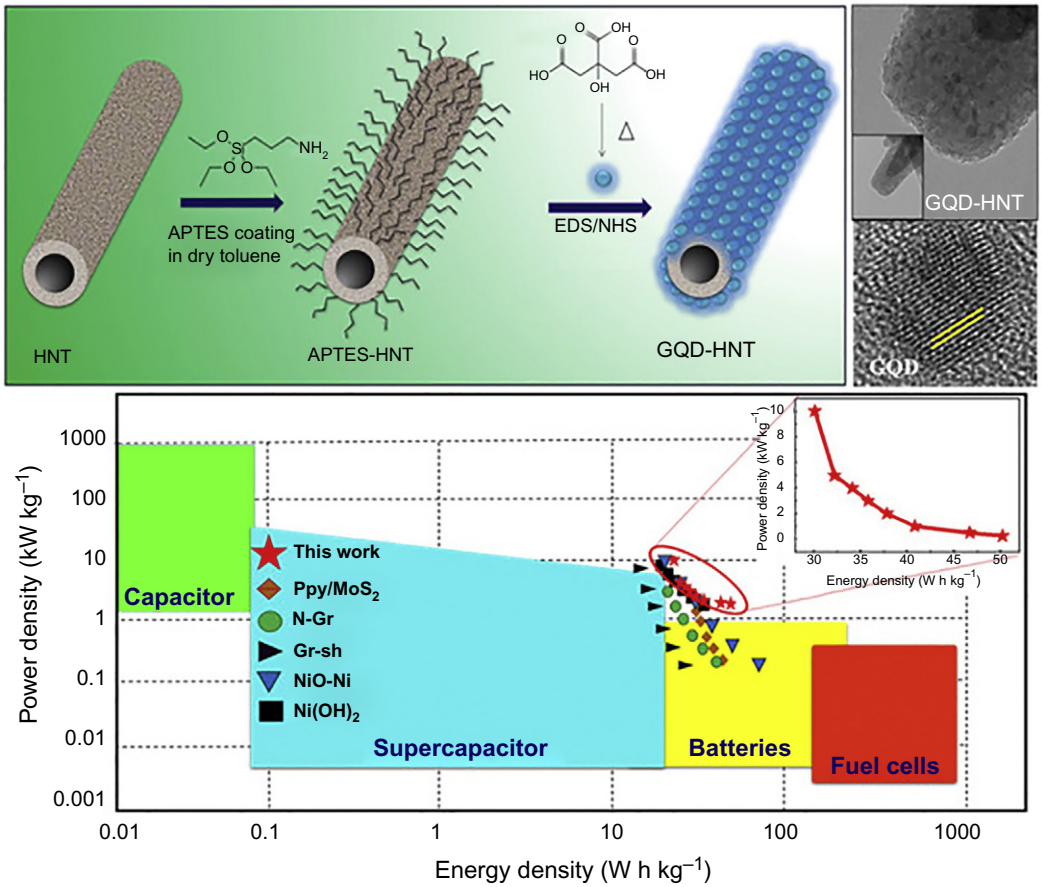

Fig. 11.11 Preparation of graphene quantum dot coated halloysite nanotubes and supercapacitor application. Reprinted with permission from A.B. Ganganboina, A.D. Chowdhury, R. Doong, A new avenue for appendage of graphene quantum dots on halloysite nanotubes as anode mmaterials for high performances supercapacitors, ACS Sustain. Chem. Eng. 5 (2017) 4930–4940. Copyright (2017) American Chemical Society.

hydrogen storage because the high-surface area and porosity provide additional binding sites on the surface and within the pores through a physical adsorption [126, 127]. Jin et al. prepared carbon/halloysite hybrids by a hydrothermal process of natural halloysite and sucrose for high-performance hydrogen storage [128]. The adsorption capacity of carbon/halloysite hybrids for hydrogen was 0.48% at 2.65 MPa and 298 K, which was better than that of pristine halloysite (0.35%) under the same conditions. The incorporation of palladium nanoparticles by hydrazine hydrate reduction reaction onto the carbon/halloysite nanocomposites might further enhance the hydrogen storage capacity to 0.58% based on the spillover mechanism. The graphene-like/clay minerals nanocomposites could be used for hydrogen storage, and the

hydrogen adsorption values referred to the carbon content of samples were calculated to be 0.2% (w/w) for graphene-like/montmorillonite and 0.4% (w/w) for graphene-like/sepiolite, respectively [123]. The graphene-like carbon derived from sepiolite exhibited a topology that favored the hydrogen-adsorption capacity compared with that from montmorillonite, which might be related to the difference in the assembly of caramel on sepiolite and montmorillonite.

11.4.3 Reinforcing Filler

Polymer materials incorporated with inorganic nanomaterials as reinforcing fillers have attracted special research interest [129, 130], and the reinforcing fillers generally include particles (e.g., silica, metal, and other organic or inorganic materials), layered materials (e.g., graphite, layered silicate), and fibrous materials (e.g., nanofibers and nanotubes) [131, 132]. Sharmila et al. investigated the effect of fillers with different dimensionality on mechanical properties of nanofiller-reinforced polyolefin elastomers including carbon nanotubes, two-dimensional clay minerals, and three-dimensional boehmite [133]. The results indicated that the reinforcing effect of the involved nanofiller followed the order: one-dimensional > two-dimensional > three-dimensional nanomaterials. The incorporation of reinforcing fillers was favorable to improve the mechanical properties of polymer materials, such as hardness, tensile modulus, strength, and toughness at both low and high temperatures. In addition, the barrier properties, thermal stability, and extinguishing characteristics of polymer materials also could be improved significantly [134], which facilitated the application of the nanocomposites in food packaging, separation membranes, adhesives, textiles, and others [135].

As reinforcing fillers, either carbon materials or clay minerals were proved to be effective to improve the mechanical properties of polymer materials [136–140]. It was believed that the combination of carbon materials and clay minerals could construct new hybrid reinforcing fillers with properties superior to individual components, due to the synergistic effect of different types of materials. According to the dimension of two individual components for formation of carbon/clay minerals nanocomposites, it can be classified as the same dimensional carbon/clay minerals filler composed of the same dimensional carbon materials and clay minerals, with the mixed dimensional one composed of different dimensional carbon materials and clay minerals.

11.4.3.1 Same Dimensional Carbon/Clay Mineral Reinforcing Filler

Carbon nanotubes/sepiolite nanocomposites were prepared by co-dispersion approach in water based on their cooperativeness [11]. After being added into polyvinyl alcohol, the elastic modulus of polyvinyl

alcohol material was greatly improved. Jiang et al. achieved simultaneous reinforcing and toughening of polyurethane composites by incorporating carbon nanotube/halloysite hybrids fillers using a simple solution-casting method [141]. The results suggested the tensile strength; Young's modulus and elongation at break of the resultant polyurethane composite were significantly improved by 140%, 35%, and 68%, respectively, after incorporation of 1 wt% carbon nanotube/halloysite hybrids.

11.4.3.2 Mixed Dimensional Carbon/Clay Mineral Reinforcing Filler

Compared with the preparation method of the same dimensional carbon/clay minerals nanocomposites, most of the mixed dimensional carbon/clay minerals hybrids were prepared by a catalytic chemical vapor deposition process, in which clay minerals were the dual carries for catalyst and carbon [142, 143]. Carbon nanotubes/montmorillonite hybrids were fabricated for reinforcing polyurethane nanocomposite foams by an in situ polymerization process, in which the hybrids were obtained by growth of carbon nanotubes on iron-impregnated montmorillonite using a chemical vapor deposition method [144]. The incorporation of 0.25% carbon nanotubes/montmorillonite hybrids enhanced the compressive modulus and compressive strength of the composites by 31% and 20%, respectively. However, the addition of excessive carbon nanotubes/montmorillonite hybrids did not improve the performance of the composite again due to the presence of agglomerates. It was worth noting that the preexfoliation of montmorillonite by the growth of carbon nanotubes on montmorillonite layers improved the interaction between the hybrid filler and polymer matrix, which further enhanced the dispersion of the hybrid filler in the polymer matrix.

The poly(ε-caprolactone) nanocomposites were also prepared by melt mixing poly(ε-caprolactone) with carbon nanotubes/montmorillonite hybrids at concentrations of 0.5, 1.0, and 2.5 wt% [145]. All nanocomposites exhibited similar stress-strain patterns with neat poly(ε-caprolactone). Although there were no chemical interactions between poly(ε-caprolactone) and carbon nanotubes/montmorillonite hybrids, the tensile strength at break enhanced after introduction of 0.5–1 wt% carbon nanotubes/montmorillonite hybrids, while Young's modulus was increased with increasing the content of carbon nanotubes/montmorillonite hybrids. However, the introduction of nanofiller presented a negative effect on thermal stability because the carbon nanotubes/montmorillonite might catalyze the decomposition of poly(ε-caprolactone) at relatively lower temperatures. In addition, Gorrasi et al. studied the effect of photo degradation on the mechanical, thermal, and electrical properties of polylactic acid reinforced with carbon nanotubes/montmorillonite [146]. Young's Modulus measurement results indicated a strong mechanical degradation with

a prolonged UV irradiation time due to the extensive macromolecular chain scission induced by the UV irradiation, but the decrease tendency of nanocomposites was smaller than that of neat polylactic acid. The degradation temperature decreased with the photoaging, while the electrical conductivity of the nanocomposites monotonically increased with a prolonged the UV irradiation time.

In addition to one-dimensional carbon nanotubes and two-dimensional clay minerals, the one-dimensional attapulgite and two-dimensional graphene oxide were also used to fabricate the mixed dimensional carbon/clay mineral hybrids, which were incorporated into epoxy composites to improve the thermal and mechanical properties [147]. A better interfacial interaction was obtained with proper attapulgite content by increasing the roughness of graphene oxide surfaces. Therefore, the remarkable enhancement of tensile properties and fracture toughness were observed after addition of the hybrids containing 1 wt% attapulgite and 0.2 wt% graphene oxide, and the Young's modulus, tensile strength, critical stress intensity factor and critical energy release rate of composites increased by 36%, 16%, 27%, and 19%, respectively.

11.4.4 Catalysis

Carbon materials and clay minerals are excellent supporters for fabrication of catalysts owing to their large specific surface area, excellent surface activity, chemical stability, and easy modification advantage [148, 149]. By contrast, the advantages and disadvantages of clay minerals and carbon materials are different. For instance, clay minerals are low-cost and naturally abundant supporters, but it is difficult to obtain high-purity minerals in nature, which limited the application of natural clay minerals in catalysis. Most carbon materials are synthesized with a relatively higher purity and unique electrical or thermal conductivity at relative harsh conditions, but their price is very high due to the low yield and complex preparation process. Therefore, the design of carbon/clay minerals nanocomposites integrated the advantages of carbon materials, and clay minerals provided a feasible way to extend their applications in catalysis field.

11.4.4.1 Photocatalysis

Carbon-based quantum dots including graphene quantum dots and carbon quantum dots, as a new class of carbon nanomaterials with sizes smaller than 10 nm, have recently been developed for catalytic applications [150, 151]. However, the small-size carbon-based quantum dots are easy to aggregate during the carbonization process, which decreases their catalytic activities. Therefore, the carbon quantum dots/attapulgite nanocomposite was prepared by a simple

impregnation method and used for photocatalytic degradation of dibenzothiophene in model gasoline under visible light irradiation, and the maximum desulfurization rate of carbon quantum dots/attapulgite nanocomposite to dibenzothiophene reached 93% [152]. In order to further enhance the photocatalytic properties of carbon quantum dots/clay minerals composites, perovskite-type oxides, for example, $SmFeO_3$ [153] or $LaCoO_3$ [154], was incorporated to construct heterojunction photocatalysts with improved photocatalytic activity.

11.4.4.2 Catalytic Synthesis and Conversion

Liquid acids (e.g., H_2SO_4, H_3PO_4, phenylsulfonic acid) were wildly used as acid catalysts in esterification, alkylation, and isomerization reaction. However, the application of liquid acids in catalysis was limited because they may cause environmental pollution and separation and corrosion problems. Thus, solid-acid catalysts attracted more attention due to their advantages, such as easy separation, low toxicity, and corrosion [155, 156]. Jiang et al. prepared sulfonated carbon/palygorskite nanocomposite catalyst via carbonization of sucrose on palygorskite followed by sulfonation with concentrated sulfuric acid [157]. The obtained nanocomposite catalysts presented large BET surface area and high catalytic activates to the esterification reaction of acetic acid and *n*-butyl alcohol.

The carbon/clay mineral nanocomposites were also used as supporters of metal nanoparticles to overcome the aggregation of particles and enhance the catalytic activity of metal catalysts [158]. Zhong et al. fabricated Sb/carbon/palygorskite (Sb/carbon/Pal) nanocomposites by a facile impregnation and in situ calcining method for catalytic reduction of 4-nitrophenol using $NaBH_4$ as reductant [159]. As shown in Fig. 11.12, the modified Pal had no catalytic activity for hydrogenation of 4-nitrophenol, and the hydrogenation performance of the as-prepared catalysts did not increase with increasing the loading amount of Sb, which might be related to the good dispersion of Sb nanoparticles on Pal. Comparatively, incorporation of Pal contributed to improve the dispersion and to control the size distribution of Sb nanoparticles; Thus, Sb/carbon/Pal nanocomposites exhibited more stable catalytic properties for reduction of 4-nitrophenol due to the strong interaction between Sb nanoparticles and Pal.

11.4.4.3 Electrocatalysis

Electrocatalysts may participate in electrochemical reactions to increase the oxidation and reduction reaction rate, which is a specific form of catalysts that work at electrode surfaces or the electrode itself. The electrocatalysts can accelerate the transferring of electrons between electrode and reactants, and/or facilitate to an intermediate

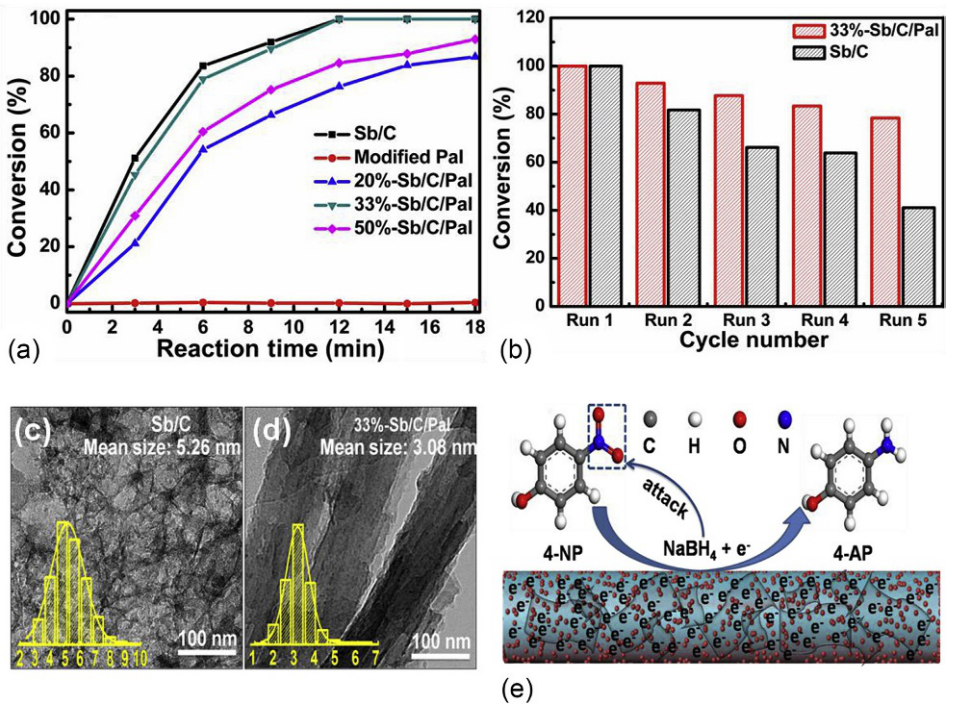

Fig. 11.12 (A) Hydrogenation conversion efficiency of 4-nitrophenol in the presence of Sb/C, modified Pal, Sb/carbon/Pal nanocomposites with different Sb loading; (B) Stability test of Sb/C and Sb/carbon/Pal nanocomposites with 33% Sb; (C) and (D) TEM images and particle-size distributions of Sb/C and Sb/carbon/Pal nanocomposites with 33% Sb after reuse for five cycles; and (E) illustration of the catalytic hydrogenation reaction mechanism for reduction of 4-NP. Reproduced with permission from L.F. Zhong, A.D. Tang, X. Wen, P. Yan, J.J. Wang, L. Tan, et al., New finding on Sb (2–3 nm) nanoparticles and carbon simultaneous anchored on the porous palygorskite with enhanced catalytic activity, J. Alloys Compd. 743 (2018) 394–402.

chemical transformation described by an overall half-reaction [160, 161]. Due to the presence of carbon species, carbon/clay minerals nanocomposites can serve as an efficient supporter of electrocatalysts. Pd nanoparticles with a diameter about 4.3 nm were anchored on a nitrogen-doped graphitic layer encapsulated palygorskite, as prepared by carbonizing the polypyrrole coated palygorskite, to form a nanocomposite electrocatalyst for oxygen reduction reaction in proton exchange membrane fuel cell [162]. The nanocomposite electrocatalysts showed superior catalytic performance and good stability compared with that of commercial Pt/C anode during oxygen-reduction reaction. It might be ascribed to the incorporation of the nitrogen atom and the acidic electronic acceptor component of SiO_2 derived from palygorskite, which made Pt nanoparticles anchored on the surface of supporter more stably by the electronic interaction between Pt and

SiO_2. Furthermore, palygorskite-hybridized carbon as supporter of electrocatalyst PtRuIr improved the electrocatalytic activity toward methanol oxidation and CO tolerance [163].

11.4.5 Sensor

Rapid and accurate evaluation of pollutants in our living environment is one of the key tasks of environmental monitoring. The chemical toxins, heavy metals, volatile organic compounds, and inorganic/organic pollutants in the environment need to be monitored constantly to safeguard the supply of secure drinking water, air, and food. Therefore, it is a great challenge to develop a sensitive and selective method to monitor these pollutants. At present, electrochemical methods have received increasing attention due to their advantages of rapid, easy operation, high sensitivity and online testing, and electrochemical sensor-based electroanalytical methods have been designed and applied in many fields, such as environmental protection, pharmaceutical monitoring, and material sciences [164–167]. However, the nanomaterials used for modification of electrodes are expensive, and thus it is indispensable to design novel electrochemical sensors with low cost and high sensitivity for the detection of pollutants. Carbon/clay mineral nanocomposites may be one of the ideal candidates due to their excellent properties. The percolation principle was used to design a chemical or gas sensor comprising a conducting phase (carbon powder) and an insulating phase (montmorillonite), whose volume increased after incorporation of a desired substance [168, 169]. Upon encounter of water vapor or volatile organochlorine compounds, a reversible resistivity change in response to the concentration of the desired substance was observed, which was mainly ascribed to the change of volume fraction of the insulating phase. Zhang et al. prepared a novel nanohybrid-sensing platform for voltammetric determination of niclosamide based on palygorskite nanorods and carboxyl functionalized graphene nanosheets [170]. The as-prepared sensor exhibited enhanced synergistically electrocatalytic ability to niclosamide in a linear range from 0.02 to 0.99 μM with low limit of detection (4.6 nM), good sensitivity, and high reproducibility.

The incorporation of conductive matrix (e.g., carbon materials) is crucial to realize the application of clay minerals in electrochemical sensors. Compared with the pristine graphene, nitrogen-doped graphene possesses remarkably enhanced properties in physics, chemistry, biology, and material science [171, 172]. Therefore, the voltammetric sensor was designed to construct for simultaneous analysis of uric acid, xanthine, and hypoxanthine based on palygorskite and nitrogen-doped graphene (Fig. 11.13) [173]. The as-prepared nanocomposites exhibited an excellent electro-catalytic activity for the electrochemical oxidation of

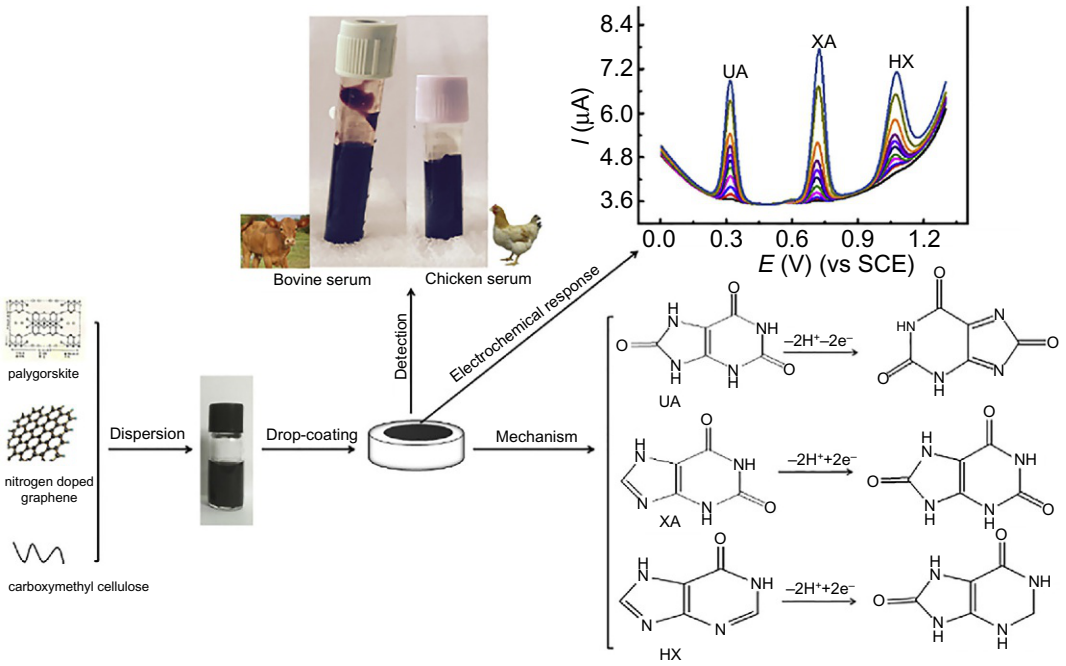

Fig. 11.13 The construction of nanocomposite electrode sensors for simultaneous voltammetric determination of uric acid, xanthine, and hypoxanthine in biological samples. Reproduced with permission from Y. Wen, J. Chang, L. Xu, X. Liao, L. Bai, Y. Lan, et al., Simultaneous analysis of uric acid, xanthine and hypoxanthine using voltammetric sensor based on nanocomposite of palygorskite and nitrogen doped graphene, J. Electroanal. Chem. 805 (2017) 159–170.

uric acid, xanthine, and hypoxanthine, which could be used to simultaneously detect uric acid, xanthine, and hypoxanthine with a wide linear of 0.5–60 μM, 0.2–20 μM, and 0.6–55 μM with a low limit of detection of 0.1, 0.05, and 0.4 μM for uric acid, xanthine, and hypoxanthine, respectively. Furthermore, the designed sensor also presented remarkable reproducibility, good selectivity, and satisfactory practicability. Thus, it is expected to be successfully applied for the simultaneous detection and analysis of uric acid, xanthine, and hypoxanthine in chicken and bovine serum samples. However, the antiinterferent ability (especially other purine derivatives) of this sensor should be further improved to make it more perfect. Due to the excellent properties, there is no doubt that clay minerals can be served as a promising candidate for electrochemical determination after being modified with conductive materials.

11.4.6 Surface and Interface Functional Materials

Inspired by animals and plants with unique repellency to water, superhydrophobic surfaces with water contact angles higher than 150

degrees have increasingly attracted attention due to the potential applications in many fields, such as self-cleaning [174], fluid transportation [175], oil/water separation [176], and antiicing [177]. In order to construct the superhydrophobic surfaces, it is indispensable to design a rough surface by modification with low-surface energy reagents. As mentioned previously, carbon/clay minerals nanocomposites exhibit a hierarchical rough structure and have great potential to design superhydrophobic coatings by moderate modification with low-surface energy reagents. Thus the durable and fluorine-free superhydrophobic coatings were fabricated combining the unique structure of carbon/palygorskite nanocomposites derived from spent bleaching earth with n-hexadecyltrimethoxysilane modification via sol-gel method [178]. It was found that the superhydrophobicity of the coating was dependent on its microstructure, which could be precisely regulated by preparation temperatures and content of carbon/palygorskite nanocomposites. The preparation temperatures mainly affected carbon content and surface roughness of carbon/palygorskite nanocomposites, while the content determined the number of carbon/palygorskite nanorods (the building blocks of superhydrophobic coating). Thus the coating prepared at the optimum conditions exhibited high water contact angles of 163.7 degree with an extremely low sliding angle (1.2 degree), featuring a high mechanical, thermal, and chemical durability.

Superhydrophobic surfaces can be easily wetted and contaminated by liquids with low-surface tension in our life, such as oils and aqueous surfactant solutions, and thus it is imperative to construct a superamphiphobic surface with unique repellency to water as well as to liquids with low surface tension, which requires surfaces with special microstructures [179] and very low-surface energy [180]. Our group also successfully prepared superamphiphobic coatings with low sliding angles based on carbon/attapulgite nanocomposites derived from the spent bleaching earth after being decorated using hydrolytic condensation of 1H, 1H, 2H, 2H-perfluorodecyltriethoxysilane and tetraethoxysilane [181]. As with the superhydrophobic coating, the surface topography of the superamphiphobic coating played an important role to adjust the superamphiphobicity of coatings, which could be easily regulated by pyrolysis temperatures of spent bleaching earth and the adding amount of carbon/attapulgite nanocomposites. As depicted in Fig. 11.14, the formed carbon nanoparticles were anchored on the surface of attapulgite nanorods during pyrolysis, and then carbon/attapulgite nanocomposites were wrapped and linked together by the fluorinated polysiloxane layer. Based on three-tier micro/nano structure originated from attapulgite nanorods, carbon nanoparticles and fluorinated polysiloxane, the obtained coatings exhibited excellent superamphiphobicity with high-contact angles (154.2 degree) and low-sliding angles (11.3 degree), as well as very good chemical and thermal stability.

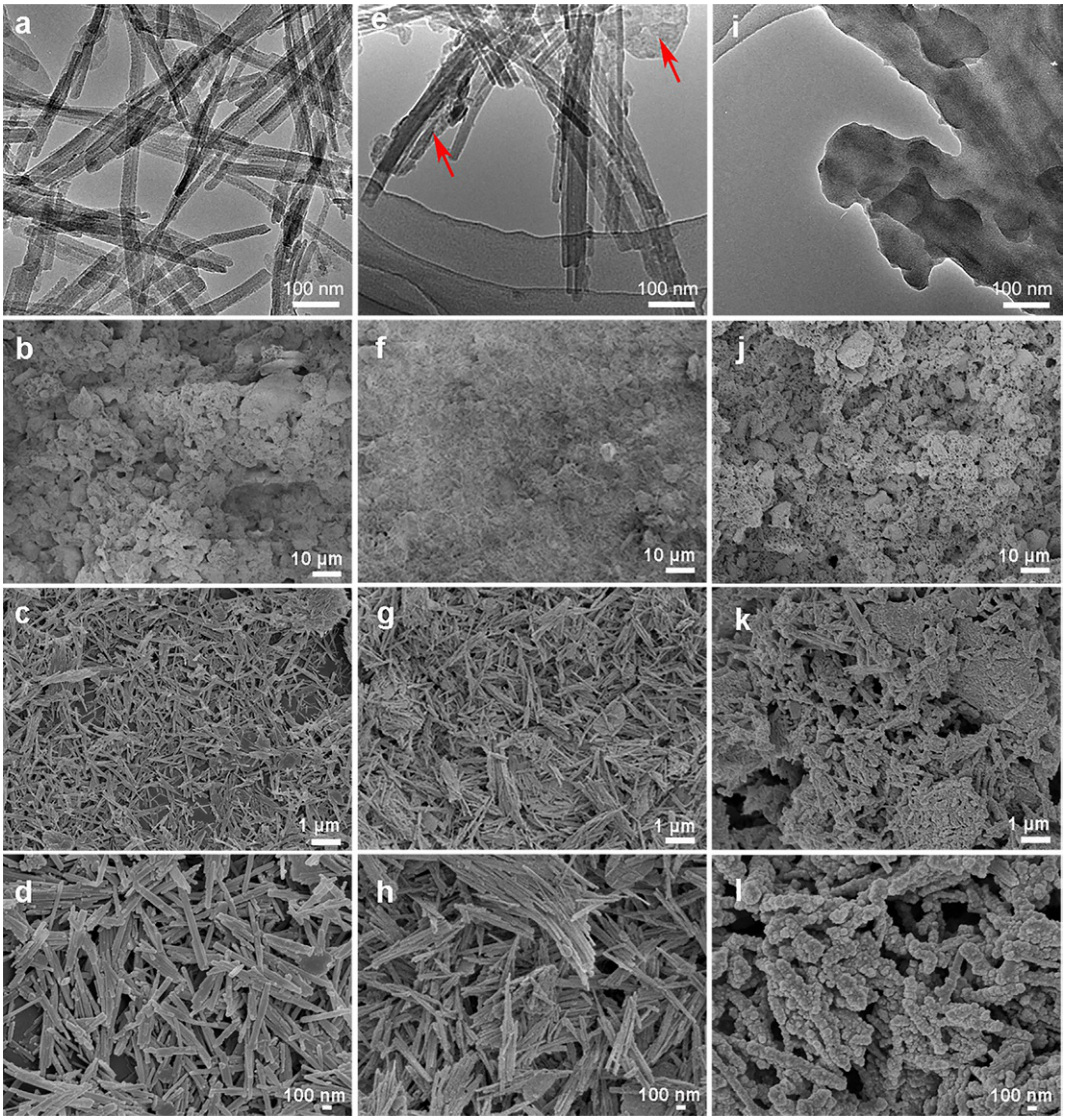

Fig. 11.14 TEM and SEM images of (A–D) attapulgite, (E–H) carbon/attapulgite nanocomposites, and (I–L) carbon/attapulgite@fluorinated polysiloxane. Reproduced with permission from S.T. Dong, B.C. Li, J.P. Zhang, A.Q. Wang, Superamphiphobic coatings with low sliding angles from attapulgite/carbon composites, Adv. Mater. Interfaces 5 (2018) 1701520.

It is well-known that the oxidation and exfoliation of graphite into graphene oxide nanosheets can enlarge the adjacent interlayer distance of graphene oxide nanosheets [182], and thus graphene oxide-based self-assemble membranes with laminate two-dimensional nanochannels between adjacent graphene oxide nanosheets have become one of

the most popular membrane materials in water treatment applications [183, 184]. It is popular to fabricate graphene oxide-based self-assembled membranes with high-water permeability and antifouling capacity based on graphene oxide and intercalated nano-units. Zhao et al. prepared a free-standing, self-assembled membrane using graphene oxide nanosheets and palygorskite nanorods by a vacuum-assisted filtration process [185]. The intercalation of palygorskite nanorods into adjacent graphene oxide nanosheets could simultaneously tailor the channel structure and surface topography of the as-prepared membranes. In the self-assemble membrane, graphene-oxide nanosheets provided the laminate structures and efficient passageways for water molecules, while the palygorskite nanorods not only enlarged mass transfer channels, but also enhanced the hydration capacity and promoted the formation of hierarchical nanostructures on membrane surfaces. All of the integrated advantages provided the membranes with robust underwater superoleophobic function and low oil-adhesive water/membrane interface. Therefore, the permeate fluxes of the obtained membranes sharply increased to 1867 $L m^{-2} h^{-1}$ (267 $L m^{-2} h^{-1}$ for graphene oxide membrane). In addition, it also exhibited excellent and universal antioil-fouling properties during oil-in-water emulsion separation in various conditions, including different concentrations, pH, or oil species.

11.4.7 Agricultural Application

As a class of functional material, biochar exhibited enormous application potential in agricultural and environmental fields [186]. Incorporation of biochar into soil not only provides the opportunities to store carbon over longer periods compared with unpyrolyzed biomass [187], but also improves the soil properties including electrical conductivity, pH, cation-exchange capacity, nutrient levels, porosity, bulk density, and microbial community structures [188, 189]. It is also favorable to alter the soil fertility and crop productivity by improving nutrient levels and decreasing the leaching of nitrogen and phosphorus [190, 191]. Moreover, biochar also can provide the additional habitats for microbial populations in soil to transform nutrients into plant-available forms, as well as reducing the risk of environmental pollutants from soils [8, 192, 193]. In addition, it was confirmed that dramatic changes in molecular structure, degradation pathways, and porosity of biochar were observed at pyrolysis temperatures ranging from 250°C to 550°C when biomass was pretreated by iron-sulfate-clay slurries compared with the untreated biochar [194]. In this process, the presence of iron clay prevented the degradation of cellulosic fraction at 250°C, but clay promoted degradation of biomass at relatively higher temperatures (350–550°C), resulting in the increase in

both the concentrations of condensed aromatic, acidic, and phenolic carbon species. Therefore, carbon/clay minerals nanocomposites may be more applicable in the agricultural field than as biomass for remediating polluted soil and decreasing the loss of nutrients [195]. The montmorillonite facilitated to the pyrolysis of bamboo biomass to form biochar at 400°C due to the catalysis action of montmorillonite as a solid acidic catalyst. The adsorption affinity of the biochar/montmorillonite nanocomposites for PO_4^{3-} was much stronger than that for NH_4^+, and the Langmuir maximum adsorption capacities toward NH_4^+ and PO_4^{3-} were 12.52 and 105.28 mg g^{-1}, respectively. The desorbed quantity of NH_4^+ and PO_4^{3-} from the nanocomposites after adsorption of NH_4^+ and PO_4^{3-} were 0.012–0.19 and 0.33–0.64 mg g^{-1}, respectively, after continuous desorption for 2–88 h. In other words, the release percentage of NH_4^+ and PO_4^{3-} was 0.30%–4.92% and 2.63%–5.09% within 88 h, respectively, indicating a reasonable release rate of NH_4^+ and PO_4^{3-}, and the superiority of the nanocomposites to fabricating slow-release fertilizers of NH_4^+ and PO_4^{3-} for application in agriculture.

11.4.8 Edible Oil Bleaching

It is well-known that the appearance and quality of edible oil must be improved before eating by treatment with a refining process including degumming, bleaching, and deodorization [196]. The bleaching treatment using activated clay with a dosage of 1%–3% is the most crucial step to the whole refining process [197]. Due to the superior performance, carbon/clay minerals nanocomposites have also been used for edible oil bleaching. Our group prepared carbon/attapulgite composite by calcining starch or chitosan/attapulgite composite precursors at 280°C, which showed the optimal performance for bleaching of palm oil due to the generation of carbon and improvement of the pore structural parameters [43, 198]. In addition, the use of carbon/attapulgite nanocomposites realized the integration of degumming and bleaching processes, and avoided the use of phosphoric acid, which must be used in conventional degumming processes. The Red value and the content of peroxide and phospholipid of palm oil decreased by 57.36%, 76.34%, and 43.11%, respectively, after bleaching.

11.5 Suggestions and Future Prospects

Owing to the attractive advantages in structure and properties, mineral materials with some special functions increasingly receive widespread attention. With the rapid development of nanoscience and nanotechnology, it has been fully possible to disperse clay minerals into nanomaterials through various physical or chemical means, and also to modify, coat, or carry various active components on the

surface of clay minerals. Given its various functions, the research and development of mineral functional materials has in recent years set off a boom, and significant progress has been made. As a material that combines the advantages of carbon materials and clay minerals, carbon/clay minerals nanocomposites have been of special interest as building blocks for fabricating various functional materials. This chapter focused on the preparation and applications of carbon/clay minerals nanocomposites, and the latest research progress has been summarized and discussed by reviewing comprehensive references combined with our group's relevant research achievements. It can be concluded that the pyrolysis process is an efficient method to fabricate carbon/clay minerals materials with the best performance and application prospects. However, the applications of carbon/clay minerals materials in the high-technology fields are still lacking, and the relevant research on this topic should be paid more attention. In addition, the current research mainly focuses on small-scale laboratory research, and there is less concern on the large-scale green preparation processes, which should be an a future focus area.

Several suggestions are proposed for the future work of carbon/clay minerals materials as follows. In the case of the common application of carbon/clay minerals nanocomposites for the removal of pollutants, it is imperative to realize the sustainable cyclic utilization of the spent adsorbents after adsorption of organic matters or heavy metal ions. The thermal regeneration has proven to be an effective strategy to recycling spent carbon/clay minerals materials containing organic matters. The obtained product may be a potential soil-remediation material integrated with multiple functions after consecutive adsorption-calcination cycles to some extent, such as the adsorption and immobilization of pollutants in soil, slow release of nutrient substances such as fertilizer, regulation of soil microbial community, and improvement of physicochemical properties of soil (e.g., electrical conductivity, pH, cation-exchange capacity, nutrient levels, porosity, etc.). Finally, in the future, we look forward to achieving "from nature, for nature, and into nature" for the comprehensive utilization of clay mineral-based materials. However, efforts are still needed to explore an eco-friendly approach to recycling the spent adsorbents after adsorption of heavy-metal ions. Perhaps, it is a feasible method to transform in situ the heavy metal ions loaded on the carbon/clay minerals nanocomposites into metal or metal-oxide nanoparticles for catalytic applications, including catalytic degradation of pollutants, various catalytic synthesis, and conversion reactions.

In addition, porous carbon materials recently have been fabricated from carbon/minerals nanocomposites after etching the clay minerals. This synthesis strategy is novel but inadvisable due to the use of the toxic chemical reagents such as hydrofluoric acid. It is suggested to design

novel functional materials based on the structures and properties of carbon/clay minerals nanocomposites, such as the confined synthesis of catalysis nanoparticles or the incorporation of sensing components within the nanopores, channels, or interlayer of carbon/clay minerals prepared using the fresh biomass or the spent clay mineral-based adsorbents. It is expected to develop new functional materials for catalytic or sensing application. Last but not least, the new applications should be extended with the development of the preparation method and functionalization or modification technology of carbon/clay minerals nanocomposites. For example, the superhydrophobic or superamphiphobic modification of carbon/clay minerals can realize their application in oil-water separation, anticorrosive coating, light-resistant and self-cleaning coating by direct surface modification without constructing a rough surface. In summary, there is no doubt that carbon/clay minerals materials must play significant roles in many areas, but serious efforts need to be focused on the development of green, facile, and low-cost technologies to realize the practical applications as soon as possible.

Acknowledgments

The authors are grateful for financial support of the Major Projects of the National Natural Science Foundation of Gansu, China (18JR4RA001), the Funds for Creative Research Groups of Gansu, China (17JR5RA306), the Youth Innovation Promotion Association of the Chinese Academy of Sciences (2017458), and the Key Research & Development Project of Gansu Provincial Sci. & Tech. Department, China (17YF1WA167).

References

[1] E. Frackowiak, F. Beguin, Carbon materials for the electrochemical storage of energy in capacitors, Carbon 39 (2001) 937–950.
[2] L.B. Wang, X.L. Hu, Recent advances in porous carbon materials for electrochemical energy storage, Chem.-Asian J. 13 (2018) 1518–1529.
[3] X.Y. Zhang, B. Gao, A.E. Creamer, C.C. Cao, Y.C. Li, Adsorption of VOCs onto engineered carbon materials: a review, J. Hazard. Mater. 338 (2017) 102–123.
[4] M.Q. Lv, L.W. Yan, C. Liu, C.J. Su, Q.L. Zhou, X. Zhang, et al., Non-covalent functionalized graphene oxide (GO) adsorbent with an organic gelator for co-adsorption of dye, endocrine-disruptor, pharmaceutical and metal ion, Chem. Eng. J. 349 (2018) 791–799.
[5] X.C. Duan, J.T. Xu, Z.X. Wei, J.M. Ma, S.J. Guo, S.Y. Wang, et al., Metal-free carbon materials for CO_2 electrochemical reduction, Adv. Mater. 29 (2017). 1701784.
[6] S.X. Dou, Y. Wang, J. Li, Z.D. Wei, Recent progress of carbon-based materials in oxygen reduction reaction catalysis, Chem. Aust. 5 (2018) 1764–1774.
[7] E. Bekyarova, Y.C. Ni, E.B. Malarkey, V. Montana, J.L. McWilliams, R.C. Haddon, et al., Applications of carbon nanotubes in biotechnology and biomedicine, J. Biomed. Nanotechnol. 1 (2005) 3–17.
[8] M. Ahmad, A.U. Rajapaksha, J.E. Lim, M. Zhang, N. Bolan, D. Mohan, et al., Biochar as a sorbent for contaminant management in soil and water: a review, Chemosphere 99 (2014) 19–33.

[9] G. Crini, P.M. Badot, Sorption Process and Pollution, Conventional and Non-Conventional Sorbents for Pollutant Removal From Wastewaters, Presses Universitaires de Franche-Comté, Besançon, 2010.
[10] Z. Wang, X.Y. Meng, J.Z. Li, X.H. Du, S.Y. Li, Z.W. Jiang, et al., A simple method for preparing carbon nanotubes/clay hybrids in water, J. Phys. Chem. C 113 (2009) 8058–8064.
[11] F.M. Fernandes, E. Ruiz-Hitzky, Assembling nanotubes and nanofibres: cooperativeness in sepiolite-carbon nanotube materials, Carbon 72 (2014) 296–303.
[12] S. Roy, S.K. Srivastava, J. Pionteck, V. Mittal, Montmorillonite-multiwalled carbon nanotube nanoarchitecture reinforced thermoplastic polyurethane, Polym. Compos. 37 (2016) 1775–1785.
[13] T. Tsoufis, V. Georgakilas, X.X. Ke, G. Van Tendeloo, P. Rudolf, D. Gournis, Incorporation of pure fullerene into organoclays: towards C60-pillared clay structures, Chem. A Eur. J. 19 (2013) 7937–7943.
[14] V.B. Yadav, R. Gadi, S. Kalra, Synthesis and characterization of novel nanocomposite by using kaolinite and carbon nanotubes, Appl. Clay Sci. 155 (2018) 30–36.
[15] K. Chen, L.R. Shi, Y.F. Zhang, Z.F. Liu, Scalable chemical-vapour-deposition growth of three-dimensional graphene materials towards energy-related applications, Chem. Soc. Rev. 47 (2018) 3018–3036.
[16] I. Ibrahim, T. Gemming, W.M. Weber, T. Mikolajick, Z.F. Liu, M.H. Rummeli, Current progress in the chemical vapor deposition of type-selected horizontally aligned single-walled carbon nanotubes, ACS Nano 10 (2016) 7248–7266.
[17] D. Gournis, M.A. Karakassides, T. Bakas, N. Boukos, D. Petridis, Catalytic synthesis of carbon nanotubes on clay minerals, Carbon 40 (2002) 2641–2646.
[18] A. Bakandritsos, A. Simopoulos, D. Petridis, Carbon nanotube growth on a swellable clay matrix, Chem. Mater. 17 (2005) 3468–3474.
[19] D. Manikandan, R.V. Mangalaraja, R. Siddheswaran, R.E. Avila, S. Ananthakumar, Fabrication of nanostructured clay-carbon nanotube hybrid nanofiller by chemical vapour deposition, Appl. Surf. Sci. 258 (2012) 4460–4466.
[20] J.Q. Nie, Q. Zhang, M.Q. Zhao, J.Q. Huang, Q.A. Wen, Y. Cui, et al., Synthesis of high quality single-walled carbon nanotubes on natural sepiolite and their use for phenol absorption, Carbon 49 (2011) 1568–1580.
[21] K. Pastorkova, K. Jesenak, M. Kadlecikova, J. Breza, M. Kolmacka, M. Caplovicova, et al., The growth of multi-walled carbon nanotubes on natural clay minerals (kaolinite, nontronite and sepiolite), Appl. Surf. Sci. 258 (2012) 2661–2666.
[22] M.Q. Zhao, J.Q. Huang, Q. Zhang, W.L. Luo, F. Wei, Improvement of oil adsorption performance by a sponge-like natural vermiculite-carbon nanotube hybrid, Appl. Clay Sci. 53 (2011) 1–7.
[23] J. Mumme, L. Eckervogt, J. Pielert, M. Diakite, F. Rupp, J. Kern, Hydrothermal carbonization of anaerobically digested maize silage, Bioresour. Technol. 102 (2011) 9255–9260.
[24] J. Fang, L. Zhan, Y. Sik Ok, B. Gao, Minireview of potential applications of hydrochar derived from hydrothermal carbonization of biomass, J. Ind. Eng. Chem. 57 (2018) 15–21.
[25] B. Hu, K. Wang, L.H. Wu, S.H. Yu, M. Antonietti, M.M. Titirici, Engineering carbon materials from the hydrothermal carbonization process of biomass, Adv. Mater. 22 (2010) 813–828.
[26] L.F. Chen, H.W. Liang, Y. Lu, C.H. Cui, S.H. Yu, Synthesis of an attapulgite clay@carbon nanocomposite adsorbent by a hydrothermal carbonization process and their application in the removal of toxic metal ions from water, Langmuir 27 (2011) 8998–9004.
[27] X.P. Wu, Q.X. Zhang, C. Liu, X.L. Zhang, D.D.L. Chung, Carbon-coated sepiolite clay fibers with acid pre-treatment as low-cost organic adsorbents, Carbon 123 (2017) 259–272.

[28] G.F. Wang, S. Wang, W. Sun, Z.M. Sun, S.L. Zheng, Synthesis of a novel illite@carbon nanocomposite adsorbent for removal of Cr(VI) from wastewater, J. Environ. Sci. 57 (2017) 62–71.
[29] Y.Q. Xu, X.P. Wu, C. Liu, P. Gao, X.L. Zhang, Organic modification of palygorskite with biomass by hydrothermal carbonization and characterization on its adsorption property, Chem. React. Eng. Technol. 29 (2013) 119–124.
[30] J. Zhang, T.F. Liu, M.X. Liu, Hydrothermal synthesis of halloysite nanotubes @ carbon nanocomposites with good biocompatibility, Microporous Mesoporous Mater. 266 (2018) 155–163.
[31] A. Sharma, V. Pareek, D.K. Zhang, Biomass pyrolysis—a review of modelling, process parameters and catalytic studies, Renew. Sustain. Energy Rev. 50 (2015) 1081–1096.
[32] X.D. Yang, F.F. Li, M.S. Xia, F. Luo, Y.S. Jiang, Investigation on the micro-structure and adsorption capacity of cellulosic biomass carbon based montmorillonite composite, Microporous Mesoporous Mater. 256 (2018) 18–24.
[33] A. Bakandritsos, E. Kouvelos, T. Steriotis, D. Petridis, Aqueous and gaseous adsorption from montmorillonite-carbon composites and from derived carbons, Langmuir 21 (2005) 2349–2355.
[34] Y.M. Wang, Y.L. Liu, Q.L. Lin, S.H. Dong, L. Xiong, Preparation and properties of montmorillonite/carbon foam nanocomposites, Appl. Clay Sci. 140 (2017) 31–37.
[35] A. Gómez-Avilés, M. Darder, P. Aranda, E. Ruiz-Hitzky, Multifunctional materials based on graphene-like/sepiolite nanocomposites, Appl. Clay Sci. 47 (2010) 203–211.
[36] E. Ruiz-Hitzky, M. Darder, F.M. Fernandes, E. Zatile, F.J. Palomares, P. Aranda, Supported graphene from natural resources: easy preparation and applications, Adv. Mater. 23 (2011) 5250–5255.
[37] Q.Z. Chen, R.L. Zhu, W.X. Deng, Y. Xu, J.X. Zhu, Q. Tao, et al., From used montmorillonite to carbon monolayer-montmorillonite nanocomposites, Appl. Clay Sci. 100 (2014) 112–117.
[38] J. Tang, L. Zong, B. Mu, Y.R. Kang, A.Q. Wang, Attapulgite/carbon composites as a recyclable adsorbent for antibiotics removal, Korean J. Chem. Eng. 35 (2018) 1650–1661.
[39] P. Anadao, I.L.R. Pajolli, E.A. Hildebrando, H. Wiebeck, Preparation and characterization of carbon/montmorillonite composites and nanocomposites from waste bleaching sodium montmorillonite clay, Adv. Powder Technol. 25 (2014) 926–932.
[40] B. Mu, A. Wang, Regeneration and recycling of spent bleaching earth, in: L. Martínez, O. Kharissova, B. Kharisov (Eds.), Handbook of Ecomaterials, Springer, Cham, 2018.
[41] J. Tang, B. Mu, M.S. Zheng, A.Q. Wang, One-step calcination of the spent bleaching earth for the efficient removal of heavy metal ions, ACS Sustain. Chem. Eng. 3 (2015) 1125–1135.
[42] J. Tang, B. Mu, L. Zong, M.S. Zheng, A.Q. Wang, Fabrication of attapulgite/carbon composites from the spent bleaching earth for the efficient adsorption of methylene blue, RSC Adv. 5 (2015) 38443–38451.
[43] G.Y. Tian, W.B. Wang, Y.F. Zhu, L. Zong, Y.R. Kang, A.Q. Wang, Carbon/attapulgite composites as recycled palm oil-decoloring and dye adsorbents, Materials 11 (2018) 86.
[44] R. Leboda, S. Chodorowski, J. Skubiszewska-Zięba, Y.I. Tarasevich, Effect of the carbonaceous matter deposition on the textural and surface properties of complex carbon-mineral adsorbents prepared on the basis of palygorskite, Colloid. Surf. A: Physicochem. Eng. Asp. 178 (2001) 113–128.
[45] K. Peng, H.M. Yang, Carbon hybridized montmorillonite nanosheets: preparation, structural evolution and enhanced adsorption performance, Chem. Commun. 53 (2017) 6085–6088.

[46] M. Danish, T. Ahmad, A review on utilization of wood biomass as a sustainable precursor for activated carbon production and application, Renew. Sustain. Energy Rev. 87 (2018) 1–21.
[47] F. Marrakchi, M. Bouaziz, B.H. Hameed, Activated carbon-clay composite as an effective adsorbent from the spent bleaching sorbent of olive pomace oil: process optimization and adsorption of acid blue 29 and methylene blue, Chem. Eng. Res. Des. 128 (2017) 221–230.
[48] X.L. Zhang, L.P. Cheng, X.P. Wu, Y.Z. Tang, Y.C. Wu, Activated carbon coated palygorskite as adsorbent by activation and its adsorption for methylene blue, J. Environ. Sci. 33 (2015) 97–105.
[49] A. Bakandritsos, T. Steriotis, D. Petridis, High surface area montmorillonite-carbon composites and derived carbons, Chem. Mater. 16 (2004) 1551–1559.
[50] W.W. Zhang, Z.B. Ren, Z.R. Ying, X.D. Liu, H. Wan, Activated nitrogen-doped porous carbon ensemble on montmorillonite for high-performance supercapacitors, J. Alloys Compd. 743 (2018) 44–51.
[51] X.P. Wu, C. Liu, H.J. Qi, X.L. Zhang, J.J. Dai, Q.X. Zhang, et al., Synthesis and adsorption properties of halloysite/carbon nanocomposites and halloysite-derived carbon nanotubes, Appl. Clay Sci. 119 (2016) 284–293.
[52] X.M. Sun, Y.D. Li, Colloidal carbon spheres and their core/shell structures with noble-metal nanoparticles, Angew. Chem. Int. Ed. 43 (2004) 597–601.
[53] Q.Z. Chen, H.M. Liu, R.L. Zhu, X. Wang, S.Y. Wang, J.X. Zhu, et al., Facile synthesis of nitrogen and sulfur co-doped graphene-like carbon materials using methyl blue/montmorillonite composites, Microporous Mesoporous Mater. 225 (2016) 137–143.
[54] K. Kinoshita, Carbon Electrochemical and Physicochemical Properties, Wiley, New York, 1988.
[55] H.P. Boehm, Some aspects of the surface chemistry of carbon blacks and other carbons, Carbon 32 (1994) 759–769.
[56] B. Sarkar, E. Liu, S. McClure, J. Sundaramurthy, M. Srinivasan, R. Naidu, Biomass derived palygorskite-carbon nanocomposites: synthesis, characterisation and affinity to dye compounds, Appl. Clay Sci. 114 (2015) 617–626.
[57] A.M. Ghaedi, A. Vafaei, Applications of artificial neural networks for adsorption removal of dyes from aqueous solution: a review, Adv. Colloid Interface Sci. 245 (2017) 20–39.
[58] K. Sharma, A.K. Dalai, R.K. Vyas, Removal of synthetic dyes from multicomponent industrial wastewaters, Rev. Chem. Eng. 34 (2018) 107–134.
[59] T. Ngulube, J.R. Gumbo, V. Masindi, A. Maity, An update on synthetic dyes adsorption onto clay based minerals: a state-of-art review, J. Environ. Manage. 191 (2017) 35–57.
[60] S. Kim, C.M. Park, M. Jang, A. Son, N. Her, M. Yu, et al., Aqueous removal of inorganic and organic contaminants by graphene-based nanoadsorbents: a review, Chemosphere 212 (2018) 1104–1124.
[61] X.P. Wu, Y.Q. Xu, X.L. Zhang, Y.C. Wu, P. Gao, Adsorption of low-concentration of methylene blue onto a palygorskite/carbon composite, New Carbon Mater. 31 (2015) 71–78.
[62] B. Mu, A.Q. Wang, Adsorption of dyes onto palygorskite and its composites: a review, J. Environ. Chem. Eng. 4 (2016) 1274–1294.
[63] B. Mu, A.Q. Wang, One-pot fabrication of multifunctional superparamagnetic attapulgite/Fe_3O_4/polyaniline nanocomposites served as adsorbent and catalyst support, J. Mater. Chem. A 3 (2015) 281–289.
[64] B. Mu, J. Tang, L. Zhang, A.Q. Wang, Preparation, characterization and application on dye adsorption of a well-defined two-dimensional superparamagnetic clay/polyaniline/Fe_3O_4 nanocomposite, Appl. Clay Sci. 132–133 (2016) 7–16.
[65] J. Tang, B. Mu, L. Zong, M.S. Zheng, A.Q. Wang, Facile and green fabrication of magnetically recyclable carboxyl-functionalized attapulgite/carbon

nanocomposites derived from spent bleaching earth for wastewater treatment, Chem. Eng. J. 322 (2017) 102–114.

[66] J. Tang, B. Mu, L. Zong, A.Q. Wang, One-step synthesis of magnetic attapulgite/carbon supported NiFe-LDHs by hydrothermal process of spent bleaching earth for pollutants removal, J. Clean. Prod. 172 (2018) 673–685.

[67] D. Bouazza, H. Miloudi, M. Adjdir, A. Tayeb, A. Boos, Competitive adsorption of Cu (II) and Zn (II) on impregnate raw Algerian bentonite and efficiency of extraction, Appl. Clay Sci. 151 (2018) 118–123.

[68] A.M. Da Costa Lopes, M. Brenner, P. Falé, L.B. Roseiro, R. Bogel-Łukasik, Extraction and purification of phenolic compounds from lignocellulosic biomass assisted by ionic liquid, polymeric resins, and supercritical CO_2, ACS Sustain. Chem. Eng. 4 (2016) 3357–3367.

[69] A. Cabrera-Codony, A. Georgi, R. Gonzalez-Olmos, H. Valdés, M.J. Martín, Zeolites as recyclable adsorbents/catalysts for biogas upgrading: removal of octamethylcyclotetrasiloxane, Chem. Eng. J. 307 (2017) 820–827.

[70] F. Sharif, L.R. Gagnon, S. Mulmi, E.P.L. Roberts, Electrochemical regeneration of a reduced graphene oxide/magnetite composite adsorbent loaded with methylene blue, Water Res. 114 (2017) 237–245.

[71] S.C.R. Marques, J.M. Marcuzzo, M.R. Baldan, A.S. Mestre, A.P. Carvalho, Pharmaceuticals removal by activated carbons: role of morphology on cyclic thermal regeneration, Chem. Eng. J. 321 (2017) 233–244.

[72] Y.Y. Gao, D.B. Zhong, D.F. Zhang, X.P. Pu, X. Shao, C.H. Su, et al., Thermal regeneration of recyclable reduced graphene oxide/Fe_3O_4 composites with improved adsorption properties, J. Chem. Technol. Biotechnol. 89 (2014) 1859–1865.

[73] E.M. Nigri, A. Bhatnagar, S.D.F. Rocha, Thermal regeneration process of bone char used in the fluoride removal from aqueous solution, J. Clean. Prod. 142 (2017) 3558–3570.

[74] E. Çalışkan, J.M. Bermúdez, J.B. Parra, J.A. Menéndez, M. Mahramanlıoğlu, C.O. Ania, Low temperature regeneration of activated carbons using microwaves: revising conventional wisdom, J. Environ. Manage. 102 (2012) 134–140.

[75] J. Tang, L. Zong, B. Mu, Y.F. Zhu, A.Q. Wang, Preparation and cyclic utilization assessment of palygorskite/carbon composites for sustainable efficient removal of methyl violet, Appl. Clay Sci. 161 (2018) 317–325.

[76] J. Tang, B. Mu, L. Zong, A.Q. Wang, From waste hot-pot oil as carbon precursor to development of recyclable attapulgite/carbon composites for wastewater treatment, J. Environ. Sci. 75 (2019) 346–358.

[77] L.H. Ai, L.L. Li, Efficient removal of organic dyes from aqueous solution with ecofriendly biomass-derived carbon@montmorillonite nanocomposites by one-step hydrothermal process, Chem. Eng. J. 223 (2013) 688–695.

[78] W.J. Liu, C. Yao, M.H. Wang, J.L. Ji, L. Ying, C.Y. Fu, Kinetics and thermodynamics characteristics of cationic yellow X-GL adsorption on attapulgite/rice hull-based activated carbon nanocomposites, Environ. Prog. Sustain. Energy 32 (2013) 655–662.

[79] Y. Yao, B. Gao, J. Fang, M. Zhang, H. Chen, Y.M. Zhou, et al., Characterization and environmental applications of clay-biochar composites, Chem. Eng. J. 242 (2014) 136–143.

[80] J.L. Yin, M.S. Pei, Y.J. He, Y.K. Du, W.J. Guo, L.Y. Wang, Hydrothermal and activated synthesis of adsorbent montmorillonite supported porous carbon nanospheres for removal of methylene blue from waste water, RSC Adv. 5 (2015) 89839–89847.

[81] Q. Zhou, Q. Gao, W.J. Luo, C.J. Yan, Z.N. Jia, P. Duan, One-step synthesis of amino-functionalized attapulgite clay nanoparticles adsorbent by hydrothermal carbonization of chitosan for removal of methylene blue from wastewater, Colloids Surf. A: Physicochem. Eng. Asp. 470 (2015) 248–257.

[82] W.J. Liu, T. Yang, J. Xu, Q. Chen, C. Yao, S.X. Zuo, et al., Preparation and adsorption property of attapulgite/carbon nanocomposite, Environ. Prog. Sustain. Energy 34 (2015) 437–444.
[83] J. Tang, B. Mu, W.B. Wang, M.S. Zheng, A.Q. Wang, Fabrication of manganese dioxide/carbon/attapulgite composites derived from spent bleaching earth for adsorption of Pb(II) and brilliant green, RSC Adv. 6 (2016) 36534–36543.
[84] G.Y. Tian, W.B. Wang, L. Zong, Y.R. Kang, A.Q. Wang, From spent dye-loaded palygorskite to a multifunctional palygorskite/carbon/Ag nanocomposite, RSC Adv. 6 (2017) 41696–41706.
[85] S. Chen, M. Zhou, H.F. Wang, T. Wang, X.S. Wang, H.B. Hou, et al., Adsorption of reactive brilliant red X-3B in aqueous solutions on clay-biochar composites from bagasse and natural attapulgite, Water 10 (2018) 703.
[86] A.A. Siyal, M.R. Shamsuddin, M.I. Khan, N.E. Rabat, M. Zulfiqar, et al., A review on geopolymers as emerging materials for the adsorption of heavy metals and dyes, J. Environ. Manage. 224 (2018) 327–339.
[87] B. Qiu, H.B. Gu, X.R. Yan, J. Guo, Y.R. Wang, D.Z. Sun, et al., Cellulose derived magnetic mesoporous carbon nanocomposites with enhanced hexavalent chromium removal, J. Mater. Chem. A 2 (2014) 17454–17462.
[88] A.S. Mohammed, A. Kapri, R. Goel, Heavy metal pollution: source, impact, and remedies, in: M. Khan, A. Zaidi, R. Goel, J. Musarrat (Eds.), Biomanagement of Metal-Contaminated Soils, Environ. Pollut., Springer, Dordrecht, 2011.
[89] F.E. Soetaredjo, Y.H. Ju, S. Ismadji, A. Ayucitra, Removal of Cu(II) and Pb(II) from wastewater using biochar-clay nanocomposite, Desalin. Water Treat. 82 (2017) 188–200.
[90] Z.H. Xiao, Q.Q. Cui, X.Y. Chen, X.L. Li, F.F. Peng, R. Zhang, et al., Magnetically separable Ni/SPL@carbon nanocomposite for removal of Pb(II) from the aqueous solution, Appl. Clay Sci. 101 (2014) 184–191.
[91] T. Zhao, Y. Yao, M.L. Wang, R.J. Chen, Y.J. Yu, F. Wu, et al., Preparation of MnO_2-modified graphite sorbents from spent Li-ion batteries for the treatment of water contaminated by lead, cadmium, and silver, ACS Appl. Mater. Interfaces 9 (2017) 25369–25376.
[92] J. Liang, X.M. Li, Z.G. Yu, G.M. Zeng, Y. Luo, L.B. Jiang, Z.X. Yang, Y.Y. Qian, H.P. Wu, Amorphous MnO_2 modified biochar derived from aerobically composted swine manure for adsorption of Pb(II) and Cd(II), ACS Sustain. Chem. Eng. 5 (2017) 5049–5058.
[93] J.B. Fei, Y. Cui, X.H. Yan, W. Qi, Y. Yang, K.W. Wang, Q. He, J.B. Li, Controlled preparation of MnO_2 hierarchical hollow nanostructures and their application in water treatment, Adv. Mater. 20 (2008) 452–456.
[94] K.C. Zhu, H.Z. Jia, F. Wang, Y.Q. Zhu, C.Y. Wang, C.Y. Ma, Efficient removal of Pb(II) from aqueous solution by modified montmorillonite/carbon composite: equilibrium, kinetics, and thermodynamics, J. Chem. Eng. Data 62 (2017) 333–340.
[95] G. Yang, Facile one-step synthetic route to mesoporous N-doped attapulgite (ATP)@carbon composite through hydrothermal carbonization and the application to adsorbing toxic metal ions, Chem. Lett. 44 (2015) 369–371.
[96] R. Zhang, C.L. Chen, J. Li, X.K. Wang, Preparation of montmorillonite@carbon composite and its application for U(VI) removal from aqueous solution, Appl. Surf. Sci. 349 (2015) 129–137.
[97] L. Hlungwane, E.L. Viljoen, V.E. Pakade, Macadamia nutshells-derived activated carbon and attapulgite clay combination for synergistic removal of Cr(VI) and Cr(III), Adsorpt. Sci. Technol. 36 (2018) 713–731.
[98] X. Liu, X.T. Xu, J. Sun, A. Alsaedi, T. Hayat, J.X. Li, X.K. Wang, Insight into the impact of interaction between attapulgite and graphene oxide on the adsorption of U(VI), Chem. Eng. J. 343 (2018) 217–224.

[99] T. Li, J.F. Shen, S.T. Huang, N. Li, M.X. Ye, Hydrothermal carbonization synthesis of a novel montmorillonite supported carbon nanosphere adsorbent for removal of Cr(VI) from waste water, Appl. Clay Sci. 93–94 (2014) 48–55.
[100] P.S. McManus, V.O. Stockwell, G.W. Sundin, A.L. Jones, Antibiotic use in plant agriculture, Annu. Rev. Phytopathol. 40 (2002) 443–465.
[101] D.L. Smith, A.D. Harris, J.A. Johnson, E.K. Silbergeld, J.G. Morris Jr., Animal antibiotic use has an early but important impact on the emergence of antibiotic resistance in human commensal bacteria, Proc. Natl. Acad. Sci. U. S. A. 99 (2002) 6434–6439.
[102] F.C. Cabello, Heavy use of prophylactic antibiotics in aquaculture: a growing problem for human and animal health and for the environment, Environ. Microbiol. 8 (2006) 1137–1144.
[103] J.L. Martinez, Environmental pollution by antibiotics and by antibiotic resistance determinants, Environ. Pollut. 157 (2009) 2893–2902.
[104] B. Li, T. Zhang, Biodegradation and adsorption of antibiotics in the activated sludge process, Environ. Sci. Technol. 44 (2010) 3468–3473.
[105] R.L. Zhang, Z.P. Zhou, A.T. Xie, J.D. Dai, J.Y. Cui, J.H. Lang, et al., Preparation of hierarchical porous carbons from sodium carboxymethyl cellulose via halloysite template strategy coupled with KOH-activation for efficient removal of chloramphenicol, J. Taiwan Inst. Chem. Eng. 80 (2017) 424–433.
[106] J. Li, K. Zhang, H. Zhang, Adsorption of antibiotics on microplastics, Environ. Pollut. 237 (2018) 460–467.
[107] B.Q. Peng, L. Chen, C.J. Que, K. Yang, F. Deng, X.Y. Deng, et al., Adsorption of antibiotics on graphene and biochar in aqueous solutions induced by π-π interactions, Sci. Rep. 6 (2016) 31920.
[108] J.H. Zhang, M.Y. Lu, J. Wan, Y.H. Sun, H.X. Lan, X.Y. Deng, Effects of pH, dissolved humic acid and Cu^{2+} on the adsorption of norfloxacin on montmorillonite-biochar composite derived from wheat straw, Biochem. Eng. J. 130 (2018) 104–112.
[109] Y. Li, Z.W. Wang, X.Y. Xie, J.M. Zhu, R.N. Li, T.T. Qin, Removal of Norfloxacin from aqueous solution by clay-biochar composite prepared from potato stem and natural attapulgite, Colloids Surf. A: Physicochem. Eng. Asp. 514 (2017) 126–136.
[110] X. Sun, C. Wang, Y. Li, W. Wang, J. We, Treatment of phenolic wastewater by combined UF and NF/RO processes, Desalination 355 (2015) 68–74.
[111] S. Mohammadi, A. Kargari, H. Sanaeepur, K. Abbassian, A. Najafi, E. Mofarrah, Phenol removal from industrial wastewaters: a short review, Desalin. Water Treat. 53 (2015) 2215–2234.
[112] L.G.C. Villegas, N. Mashhadi, M. Chen, D. Mukherjee, K.E. Taylor, N. Biswas, A short review of techniques for phenol removal from wastewater, Curr. Pollution Rep. 2 (2016) 157–167.
[113] S.V. Badmaeva, S.T. Khankhasaeva, Regularities of phenol adsorption from aqueous solutions on carbon-mineral materials obtained from bentonite clay, Colloid J. 77 (2015) 685–691.
[114] X.P. Wu, P. Gao, X.L. Zhang, G.P. Jin, Y.Q. Xu, Y.C. Wu, Synthesis of clay/carbon adsorbent through hydrothermal carbonization of cellulose on palygorskite, Appl. Clay Sci. 95 (2014) 60–66.
[115] M. Yu, Y.Y. Han, J. Li, L.J. Wang, Magnetic carbon aerogel pyrolysis from sodium carboxymethyl cellulose/sodium montmorillonite composite aerogel for removal of organic contamination, J. Porous. Mater. 25 (2018) 657–664.
[116] D.B. Kong, Y. Gao, Z.C. Xiao, X.H. Xu, X.L. Li, L.J. Zhi, Rational design of carbon-rich materials for energy storage and conversion, Adv. Mater. 30 (2018) 1804973.
[117] C. Acar, A comprehensive evaluation of energy storage options for better sustainability, Int. J. Energy Res. 42 (2018) 3732–3746.

[118] W.B. Zhang, B. Mu, A.Q. Wang, S.J. Shao, Attapulgite oriented carbon/polyaniline hybrid nanocomposites for electrochemical energy storage, Synth. Met. 192 (2014) 87–92.
[119] W.B. Zhang, B. Mu, A.Q. Wang, Halloysite nanotubes induced synthesis of carbon/manganese dioxide coaxial tubular nanocomposites as electrode materials for supercapacitors, J. Solid State Electrochem. 19 (2015) 1257–1263.
[120] B. Mu, W.B. Zhang, W.B. Xu, A.Q. Wang, Hollowed-out tubular carbon@MnO_2 hybrid composites with controlled morphology derived from kapok fibers for supercapacitor electrode materials, Electrochim. Acta 178 (2015) 709–720.
[121] A.B. Ganganboina, A.D. Chowdhury, R. Doong, A new avenue for appendage of graphene quantum dots on halloysite nanotubes as anode mmaterials for high performances supercapacitors, ACS Sustain. Chem. Eng. 5 (2017) 4930–4940.
[122] C. Ruiz-Garcia, R. Jimenez, J. Perez-Carvajal, A. Berenguer-Murcia, M. Darder, P. Aranda, et al., Graphene-clay based nanomaterials for clean energy storage, Sci. Adv. Mater. 6 (2014) 151–158.
[123] C. Ruiz-García, J. Pérez-Carvajal, A. Berenguer-Murcia, M. Darder, P. Aranda, D. Cazorla-Amorós, E. Ruiz-Hitzky, Clay-supported graphene materials: application to hydrogen storage, Phys. Chem. Chem. Phys. 15 (2013) 18635–18641.
[124] M. Dresselhaus, I. Thomas, Alternative energy technologies, Nature 414 (2001) 332–337.
[125] J. Yang, A. Sudik, C. Wolverton, High capacity hydrogen storage materials: attributes for automotive applications and techniques for materials discovery, Chem. Soc. Rev. 39 (2010) 656–675.
[126] X.B. Yu, Z.W. Tang, D.L. Sun, L.Z. Ouyang, M. Zhu, Recent advances and remaining challenges of nanostructured materials for hydrogen storage applications, Prog. Mater. Sci. 88 (2017) 1–48.
[127] R. Nagar, B.P. Vinayan, S.S. Samantaray, S. Ramaprabhu, Recent advances in hydrogen storage using catalytically and chemically modified graphene nanocomposites, J. Mater. Chem. A 5 (2017) 22897–22912.
[128] J. Jin, L.J. Fu, H.M. Yang, J. Ouyang, Carbon hybridized halloysite nanotubes for high-performance hydrogen storage capacities, Sci. Rep. 5 (2015) 12429.
[129] C.E. Powell, G.W. Beall, Physical properties of polymer/clay nanocomposites, Curr. Opin. Solid State Mater. Sci. 10 (2006) 73–80.
[130] F. Gao (Ed.), Advances in Polymer Nanocomposites: Types and Applications, Series in Composites Science and Engineering, Woodhead Publishing, 2012.
[131] S.S. Ray, M. Okamoto, Polymer/layered silicate nanocomposites: a review from preparation to processing, Prog. Polym. Sci. 28 (2003) 1539–1641.
[132] R. Adhikari, G.H. Michler, Polymer nanocomposites characterization by microscopy, J. Macromol. Sci. C: Polym. Rev. J. 49 (2009) 141–180.
[133] P. Sharmila, L. Ralf, H.L. Hong, G. Wolfgang, R. Hans-Joachim, A. Rameshwar, Effect of filler dimensionality on mechanical properties of nanofiller reinforced polyolefin elastomers, ISRN Polym. Sci. 2013 (2013) 284504.
[134] M. Alexandre, P. Dubois, Polymer-layered silicate nanocomposites: preparation, properties and uses of a new class of materials, Mater. Sci. Eng. R: Rep. 28 (2000) 1–63.
[135] E.T. Thostension, L. Chunyu, T.W. Chou, Nanocomposites in context, Compos. Sci. Technol. 65 (2005) 491–516.
[136] I.Y. Phang, L. Shen, S.Y. Chow, W.D. Zhang, Morphology and mechanical properties of multiwalled carbon nanotubes reinforced nylon-6 composites, Macromolecules 37 (2004) 7214–7222.
[137] J.A. Puértolas, M. Castro, J.A. Morris, R. Ríosa, A. Ansón-Casaosc, Tribological and mechanical properties of graphene nanoplatelet/PEEK composites, Carbon 141 (2019) 107–122.

[138] E. Bilotti, R. Zhang, H. Deng, F. Quero, H.R. Fischer, T. Peijs, Sepiolite needle-like clay for PA6 nanocomposites: an alternative to layered silicates? Compos. Sci. Technol. 69 (2009) 2587–2595.
[139] L. Bokobza, E. Leroy, V. Lalanne, Effect of filling mixtures of sepiolite and a surface modified fumed silica on the mechanical and swelling behavior of a styrene-butadiene rubber, Eur. Polym. J. 45 (2009) 996–1001.
[140] B. Xu, W.M. Huang, Y.T. Pei, Z.G. Chen, A. Kraft, R. Reuben, et al., Mechanical properties of attapulgite clay reinforced polyurethane shape-memory nanocomposites, Eur. Polym. J. 45 (2009) 1904–1911.
[141] L. Jiang, C. Zhang, M.K. Liu, Z. Yang, W.W. Tjiu, T.X. Liu, Simultaneous reinforcement and toughening of polyurethane composites with carbon nanotube/halloysite nanotube hybrids, Compos. Sci. Technol. 91 (2014) 98–103.
[142] G. Gorrasi, S. D'Ambrosio, G. Patimo, R. Pantani, Hybrid clay-carbon nanotube/PET composites: preparation, processing, and analysis of physical properties, J. Appl. Polym. Sci. 131 (2014) 40441.
[143] L. Madaleno, R. Pyrz, L.R. Jensen, J.J.C. Pinto, A.B. Lopes, V. Dolomanova, et al., Synthesis and characterization of montmorillonite-carbon nanotubes hybrid fillers for nanocomposites, Polym. Polym. Compos. 20 (2012) 693–700.
[144] L. Madaleno, R. Pyrz, A. Crosky, L.R. Jensen, J.C.M. Rauhe, V. Dolomanova, et al., Processing and characterization of polyurethane nanocomposite foam reinforced with montmorillonite-carbon nanotube hybrids, Compos. A: Appl. Sci. Manuf. 44 (2013) 1–7.
[145] Z. Terzopoulou, D.N. Bikiaris, K.S. Triantafyllidis, G. Potsi, D. Gournis, G.Z. Papageorgiou, P. Rudolf, Mechanical, thermal and decomposition behavior of poly(epsilon-caprolactone) nanocomposites with clay-supported carbon nanotube hybrids, Thermochim. Acta 642 (2016) 67–80.
[146] G. Gorrasi, C. Milone, E. Piperopoulos, M. Lanza, A. Sorrentino, Hybrid clay mineral-carbon nanotube-PLA nanocomposite films: preparation and photodegradation effect on their mechanical, thermal and electrical properties, Appl. Clay Sci. 71 (2013) 49–54.
[147] R.G. Wang, Z. Li, W.B. Liu, W.C. Jiao, L.F. Hao, F. Yang, Attapulgite-graphene oxide hybrids as thermal and mechanical reinforcements for epoxy composites, Compos. Sci. Technol. 87 (2013) 29–35.
[148] M. Massaro, C.G. Colletti, G. Lazzara, S. Milioto, R. Noto, S. Riela, Halloysite nanotubes as support for metal-based catalysts, J. Mater. Chem. A 5 (2017) 13276–13293.
[149] S. Samad, K.S. Loh, W.Y. Wong, T.K. Lee, J. Sunarso, S.T. Chong, et al., Carbon and non-carbon support materials for platinum-based catalysts in fuel cells, Int. J. Hydrogen Energy 43 (2018) 7823–7854.
[150] Y.F. Wang, A.G. Hu, Carbon quantum dots: synthesis, properties and applications, J. Mater. Chem. C 2 (2014) 6921–6939.
[151] H.T. Li, R.H. Liu, W.Q. Kong, J. Liu, Y. Liu, et al., Carbon quantum dots with photo-generated proton property as efficient visible light controlled acid catalyst, Nanoscale 6 (2014) 867–873.
[152] S.J. Ma, X.Z. Li, X.W. Lu, S.X. Zuo, Z.Y. Li, C. Yao, Carbon quantum dots/attapulgite nanocomposites with enhanced photocatalytic performance for desulfurization, J. Mater. Sci. Mater. Electron. 29 (2018) 2709–2715.
[153] X.Z. Li, H.Y. Shi, T.S. Wang, Y.Y. Zhang, S.X. Zuo, S.P. Luo, et al., Photocatalytic removal of NO by Z-scheme mineral based heterojunction intermediated by carbon quantum dots, Appl. Surf. Sci. 456 (2018) 835–844.
[154] W. Zhu, X.Z. Li, Graphene quantum dots/$LaCoO_3$/attapulgite heterojunction photocatalysts with improved photocatalytic activity, Appl. Phys. A: Mater. 123 (2017) 272.

[155] L.A.S. Do Nascimento, R.S. Angélica, C.E.F. da Costa, J.R. Zamian, G.N. da Rocha Filho, Comparative study between catalysts for esterification prepared from kaolins, Appl. Clay Sci. 51 (2011) 267–273.
[156] K. Nakajima, M. Hara, Amorphous carbon with $-SO_3H$ groups as a solid Brønsted acid catalyst, ACS Catal. 2 (2012) 1296–1304.
[157] J.L. Jiang, Y. Xu, C.S. Duanmu, X. Gu, J. Chen, Preparation and catalytic properties of sulfonated carbon-palygorskite solid acid catalyst, Appl. Clay Sci. 95 (2014) 260–264.
[158] K. Ikeue, S. Mizukami, A. Kuroda, S. Hamada, A. Hongo, M. Masato, Noble-metal-containing nanoporous carbon synthesized within the inter-layer space of montmorillonite and its catalytic property, Appl. Catal. A: Gen. 351 (2008) 68–74.
[159] L.F. Zhong, A.D. Tang, X. Wen, P. Yan, J.J. Wang, L. Tan, et al., New finding on Sb (2–3 nm) nanoparticles and carbon simultaneous anchored on the porous palygorskite with enhanced catalytic activity, J. Alloys Compd. 743 (2018) 394–402.
[160] Z.F. Huang, J. Wang, Y.C. Peng, C.Y. Jung, A. Fisher, X. Wang, Design of efficient bifunctional oxygen reduction/evolution electrocatalyst: recent advances and perspectives, Adv. Energy Mater. 7 (2017). 1700544.
[161] N. Shaari, S.K. Kamarudin, Graphene in electrocatalyst and proton conductiong membrane in fuel cell applications: an overview, Renew. Sustain. Energy Rev. 69 (2017) 862–870.
[162] R.F. Wang, J.C. Jia, H. Li, X.S. Li, H. Wang, Y.M. Chang, et al., Nitrogen-doped carbon coated palygorskite as an efficient electrocatalyst support for oxygen reduction reaction, Electrochim. Acta 56 (2011) 452–4531.
[163] H. Wang, R. Luo, S. Ji, V. Linkov, R. Wang, Palygorskite hybridized carbon nanocomposite as PtRuIr support for the methanol oxidation reaction, Fuel Cell 14 (2014) 42–48.
[164] Y. Yao, H. Wu, J.F. Ping, Simultaneous determination of Cd(II) and Pb(II) ions in honey and milk samples using a single-walled carbon nanohorns modified screen-printed electrochemical sensor, Food Chem. 274 (2019) 8–15.
[165] K.Y. Goud, S.K. Kalisa, V. Kumar, Y.F. Tsang, S.E. Lee, K.V. Gobi, et al., Progress on nanostructured electrochemical sensors and their recognition elements for detection of mycotoxins: a review, Biosens. Bioelectron. 121 (2018) 205–222.
[166] H. Karimi-Maleh, A.F. Shojaei, K. Tabatabaeian, F. Karimi, S. Shakeri, R. Moradi, Simultaneous determination of 6-mercaptopruine, 6-thioguanine and dasatinib as three important anticancer drugs using nanostructure voltammetric sensoremploying Pt/MWCNTs and 1-butyl-3-methylimidazolium hexafluoro phosphate, Biosens. Bioelectron. 86 (2016) 879–884.
[167] G.X. Wang, A. Morrin, M.R. Li, N.Z. Liu, X.L. Luo, Nanomaterial-doped conducting polymers for electrochemical sensors and biosensors, J. Mater. Chem. B 6 (2018) 4173–4190.
[168] I. Tsuyumoto, Y. Iida, Percolation-type chemical sensor: electrical- and humidity-sensing properties of carbon-montmorillonite composites, Int. J. Appl. Ceram. Technol. 8 (2011) 793–799.
[169] I. Tsuyumoto, Y. Iida, H. Hori, Gas sensor for volatile organochlorine compounds using percolation conduction of organic montmorillonite-carbon composites, Int. J. Appl. Ceram. Technol. 8 (2011) 1408–1413.
[170] Z.X. Zhang, Y.Y. Yao, J.K. Xu, Y.P. Wen, J. Zhang, W.C. Ding, Nanohybrid sensor based on carboxyl functionalized graphene dispersed palygorskite for voltammetric determination of niclosamide, Appl. Clay Sci. 143 (2017) 57–66.
[171] H.F. Xu, L.B. Ma, Z. Jin, Nitrogen-doped graphene: synthesis, characterizations and energy applications, J. Energy Chem. 27 (2018) 146–160.

[172] Y.T. Wu, W. Lei, M.Z. Xia, F.Y. Wang, C.W. Li, C. Zhang, et al., Simultaneous electrochemical sensing of hydroquinone and catechol using nanocomposite based on palygorskite and nitrogen doped graphene, Appl. Clay Sci. 162 (2018) 38–45.
[173] Y. Wen, J. Chang, L. Xu, X. Liao, L. Bai, Y. Lan, et al., Simultaneous analysis of uric acid, xanthine and hypoxanthine using voltammetric sensor based on nanocomposite of palygorskite and nitrogen doped graphene, J. Electroanal. Chem. 805 (2017) 159–170.
[174] M. Long, S. Peng, W. Deng, X. Miao, N. Wen, Q. Zhou, et al., A robust superhydrophobic PDMS@$ZnSn(OH)_6$ coating with under-oil self-cleaning and flame retardancy, J. Mater. Chem. A 5 (2017) 22761–22771.
[175] C. Yuan, M. Huang, X. Yu, Y. Ma, X. Luo, A simple approach to fabricate the rose petal-like hierarchical surfaces for droplet transportation, Appl. Surf. Sci. 385 (2016) 562–568.
[176] L. Wu, L.X. Li, B.C. Li, J.P. Zhang, A.Q. Wang, Magnetic, durable, and superhydrophobic polyurethane@Fe_3O_4@SiO_2@fluoropolymer sponges for selective oil absorption and oil/water separation, ACS Appl. Mater. Interfaces 7 (2015) 4936–4946.
[177] A.M. Emelyanenko, L.B. Boinovich, A.A. Bezdomnikov, E.V. Chulkova, K.A. Emelyanenko, Reinforced superhydrophobic coating on silicone rubber for longstanding anti-icing performance in severe conditions, ACS Appl. Mater. Interfaces 9 (2017) 24210–24219.
[178] P.L. Zhang, S.T. Dong, B.C. Li, X.D. Wei, J.P. Zhang, Durable and fluorine-free superhydrophobic coatings from spent bleaching earth, Appl. Clay Sci. 157 (2018) 237–247.
[179] H.J. Butt, C. Semprebon, P. Papadopoulos, D. Vollmer, M. Brinkmann, M. Ciccotti, Design principles for superamphiphobic surfaces, Soft Matter 9 (2013) 418–428.
[180] J.P. Zhang, S. Seeger, Superoleophobic coatings with ultralow sliding angles based on silicone nanofilaments, Angew. Chem. Int. Ed. 50 (2011) 6652–6656.
[181] S.T. Dong, B.C. Li, J.P. Zhang, A.Q. Wang, Superamphiphobic coatings with low sliding angles from attapulgite/carbon composites, Adv. Mater. Interfaces 5 (2018) 1701520.
[182] F. Perreault, A. Fonseca de Faria, M. Elimelech, Environmental applications of graphene-based nanomaterials, Chem. Soc. Rev. 44 (2015) 5861–5896.
[183] C.N. Yeh, K. Raidongia, J. Shao, Q.H. Yang, J. Huang, On the origin of the stability of graphene oxide membranes in water, Nat. Chem. 7 (2015) 166–170.
[184] R.K. Joshi, P. Carbone, F.C. Wang, V.G. Kravets, Y. Su, I.V. Grigorieva, et al., Precise and ultrafast molecular sieving through graphene oxide membranes, Science 343 (2014) 752–754.
[185] X.T. Zhao, Y.L. Su, Y.A. Liu, Y.F. Lip, Z.Y. Jiang, Free-standing graphene oxide-palygorskite nanohybrid membrane for oil/water separation, ACS Appl. Mater. Interfaces 8 (2016) 8247–8256.
[186] M.X. Guo, Z.Q. He, S.M. Uchimiya (Eds.), Agricultural and Environmental Applications of Biochar: Advances and Barriers, SSSA Special Publication, vol. 63, Soil Science Society of America, Inc., Madison, 2016.
[187] Y. Sheng, L. Zhu, Biochar alters microbial community and carbon sequestration potential across different soil pH, Sci. Total Environ. 622 (2018) 1391–1399.
[188] H. Blanco-Canqui, Biochar and soil physical properties, Soil Sci. Soc. Am. J. 81 (2017) 687–692.
[189] R.Y. Shi, J.Y. Li, J. Jiang, M.A. Kamran, R.K. Xu, W. Qian, Incorporation of corn straw biochar inhibited the re-acidification of four acidic soils derived from different parent materials, Environ. Sci. Pollut. Res. 25 (2018) 9662–9672.
[190] Z. Liu, T. He, T. Cao, T. Yang, J. Meng, W. Chen, Effects of biochar application on nitrogen leaching, ammonia volatilization and nitrogen use efficiency in two distinct soils, J. Soil Sci. Plant Nutr. 17 (2017) 515–528.

[191] Y. Wang, Y. Liu, R. Liu, A. Zhang, S. Yang, H. Liu, et al., Biochar amendment reduces paddy soil nitrogen leaching but increases net global warming potential in Ningxia irrigation, China, Sci. Rep. 7 (2017) 1592–1602.
[192] S. Bashir, J. Zhu, Q. Fu, H. Hu, Cadmium mobility, uptake and anti-oxidative response of water spinach (Ipomoea aquatic) under rice straw biochar, zeolite and rock phosphate as amendments, Chemosphere 194 (2018) 579–587.
[193] M. Shaaban, L.V. Zwieten, S. Bashir, A. Younas, A. Núñez-Delgado, M.A. Chhajro, et al., A concise review of biochar application to agricultural soils to improve soil conditions and fight pollution, J. Environ. Manage. 228 (2018) 429–440.
[194] A. Rawal, S.D. Joseph, J.M. Hook, C.H. Chia, P.R. Munroe, S. Donne, et al., Mineral-biochar composites: molecular structure and porosity, Environ. Sci. Technol. 50 (2016) 7706–7714.
[195] L. Chen, X.L. Chen, C.H. Zhou, H.M. Yang, S.F. Ji, D.S. Tong, et al., Environmental-friendly montmorillonite-biochar composites: facile production and tunable adsorption-release of ammonium and phosphate, J. Clean. Prod. 156 (2017) 648–659.
[196] B.M.Z. Rohani, Process Design in Degumming and Bleaching of Palm Oil, Faculty of Chemical and Natural Resources Engineering, University Teknologi Malaysia, 2006.
[197] G.Y. Tian, W.B. Wang, Y.R. Kang, A.Q. Wang, Study on thermal activated sepiolite for enhancing decoloration of crude palm oil, J. Therm. Anal. Calorim. 117 (2014) 1211–1219.
[198] G.Y. Tian, W.B. Wang, B. Mu, Y.R. Kang, A.Q. Wang, Facile fabrication of carbon/attapulgite composite for bleaching of palm oil, J. Taiwan Inst. Chem. Eng. 50 (2015) 252–258.